values of v_i, θ_i and v_j, θ_j. The nodal forces $F_{y,i}$ and M_i are then obtained from Eq. (17.31) if the beam is aligned with the x axis. Hence

$$\left.\begin{aligned} F_{y,i} &= EI\left(\frac{12}{L^3}v_i - \frac{6}{L^2}\theta_i - \frac{12}{L^3}v_j - \frac{6}{L^2}\theta_j\right) \\ M_i &= EI\left(-\frac{6}{L^2}v_i + \frac{4}{L}\theta_i + \frac{6}{L^2}v_j + \frac{2}{L}\theta_j\right) \end{aligned}\right\} \tag{17.35}$$

Similar expressions are obtained for the forces at node j. From Fig. 17.6 we see that the shear force S_y and bending moment M in the beam are given by

$$\left.\begin{aligned} S_y &= F_{y,i} \\ M &= F_{y,i}x + M_i \end{aligned}\right\} \tag{17.36}$$

Substituting Eq. (17.35) into Eq. (17.36) and expressing in matrix form yields

$$\begin{Bmatrix} S_y \\ M \end{Bmatrix} = EI\begin{bmatrix} \frac{12}{L^3} & -\frac{6}{L^2} & -\frac{12}{L^3} & -\frac{6}{L^2} \\ \frac{12}{L^3}x - \frac{6}{L^2} & -\frac{6}{L^2}x + \frac{4}{L} & -\frac{12}{L^3}x + \frac{6}{L^2} & -\frac{6}{L^2}x + \frac{2}{L} \end{bmatrix}\begin{Bmatrix} v_i \\ \theta_i \\ v_j \\ \theta_j \end{Bmatrix} \tag{17.37}$$

The matrix analysis of the beam in Fig. 17.6 is based on the condition that no external forces are applied between the nodes. Obviously in a practical case a beam supports a variety of loads along its length and therefore such beams must be idealized into a number of *beam-elements* for which the above condition holds. The idealization is accomplished by merely specifying nodes at points along the beam such that any element lying between adjacent nodes carries, at the most, a uniform shear and a linearly varying bending moment. For example, the beam of Fig. 17.7 would be idealized into beam-elements 1–2, 2–3 and 3–4 for which the unknown nodal displacements are v_2, θ_2, θ_3, v_4 and θ_4 ($v_1 = \theta_1 = v_3 = 0$).

Beams supporting distributed loads require special treatment in that the distributed load is replaced by a series of statically equivalent point loads at a selected number of nodes. Clearly the greater the number of nodes chosen, the more accurate but more complicated and therefore time consuming will be the analysis. Figure 17.8 shows a typical idealization of a beam supporting a uniformly distributed load. The method of idealization may be found in specialist texts on matrix analysis.

Many simple beam problems may be idealized into a combination of two beam-elements and three nodes. A few examples of such beams are shown in Fig. 17.9. If we therefore assemble a stiffness matrix for the general case of a two beam-element system we may use it to solve a variety of problems simply by inserting the appropriate loading and support conditions. Consider the assemblage of two

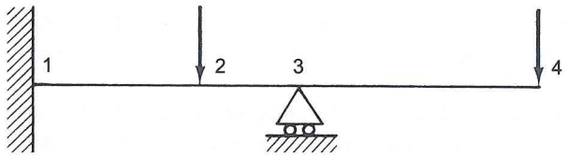

FIGURE 17.7

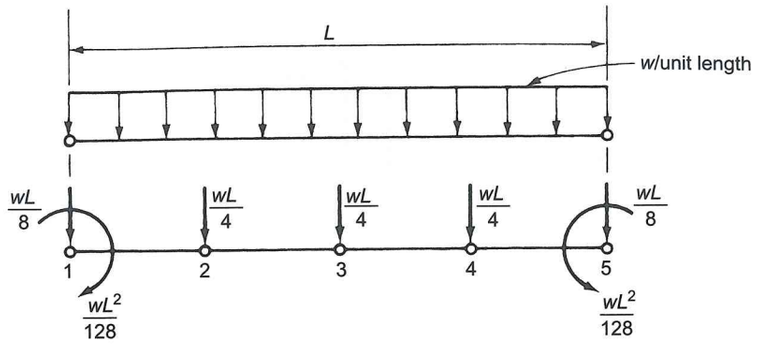

FIGURE 17.8

Idealization of a beam supporting a uniformly distributed load.

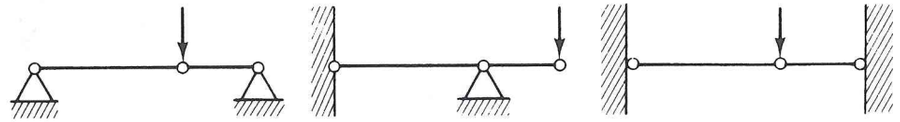

FIGURE 17.9

Idealization of beams into beam-elements.

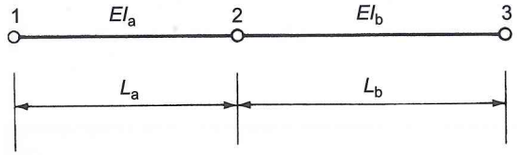

FIGURE 17.10

Assemblage of two beam-elements.

beam-elements shown in Fig. 17.10. The stiffness matrices for the beam-elements 1–2 and 2–3 are obtained from Eq. (17.31); thus

$$[K_{12}] = EI_a\begin{array}{c} \\ v_1 \\ \theta_1 \\ v_2 \\ \theta_2 \end{array}\begin{array}{c} \begin{array}{cccc} v_1 & \theta_1 & v_2 & \theta_2 \end{array} \\ \begin{bmatrix} 12/L_a^3 & -6/L_a^2 & -12/L_a^3 & -6/L_a^2 \\ -6/L_a^2 & 4/L_a & 6/L_a^2 & 2/L_a \\ -12/L_a^3 & 6/L_a^2 & 12/L_a^3 & 6/L_a^2 \\ -6/L_a^2 & 2/L_a & 6/L_a^2 & 4/L_a \end{bmatrix} \end{array} \tag{17.38}$$

$$= EI_a\begin{bmatrix} k_{11} & k_{12} \\ k_{21} & k_{22} \end{bmatrix}$$

$$[K_{23}] = EI_b \begin{array}{c} \\ v_2 \\ \theta_2 \\ v_3 \\ \theta_3 \end{array} \begin{array}{c} \begin{array}{cccc} v_2 & \theta_2 & v_3 & \theta_3 \end{array} \\ \begin{bmatrix} 12/L_b^3 & -6/L_b^2 & -12/L_b^3 & -6/L_b^2 \\ & k_{22} & & k_{23} \\ -6/L_b^2 & 4/L_b & 6/L_b^2 & 2/L_b \\ -12/L_b^3 & 6/L_b^2 & 12/L_b^3 & 6/L_b^2 \\ & k_{32} & & k_{33} \\ -6/L_b^2 & 2/L_b & 6/L_b^2 & 4/L_b \end{bmatrix} \end{array} \tag{17.39}$$

The complete stiffness matrix is formed by superimposing $[K_{12}]$ and $[K_{23}]$ as described in Ex. 17.1. Hence

$$[K] = E \begin{bmatrix} \frac{12I_a}{L_a^3} & -\frac{6I_a}{L_a^2} & -\frac{12I_a}{L_a^3} & -\frac{6I_a}{L_a^2} & 0 & 0 \\ -\frac{6I_a}{L_a^2} & \frac{4I_a}{L_a} & \frac{6I_a}{L_a^2} & \frac{2I_a}{L_a^2} & 0 & 0 \\ -\frac{12I_a}{L_a^3} & \frac{6I_a}{L_a^2} & 12\left(\frac{I_a}{L_a^3}+\frac{I_b}{L_b^3}\right) & 6\left(\frac{I_a}{L_a^2}-\frac{I_b}{L_b^2}\right) & -\frac{12I_b}{L_b^3} & -\frac{6I_b}{L_b^2} \\ -\frac{6I_a}{L_a^2} & \frac{2I_a}{L_a} & 6\left(\frac{I_a}{L_a^2}-\frac{I_b}{L_b^2}\right) & 4\left(\frac{I_a}{L_a}+\frac{I_b}{L_b}\right) & \frac{6I_b}{L_b^2} & \frac{2I_b}{L_b} \\ 0 & 0 & -\frac{12I_b}{L_b^3} & \frac{6I_b}{L_b^2} & \frac{12I_b}{L_b^3} & \frac{6I_b}{L_b^2} \\ 0 & 0 & -\frac{6I_b}{L_b^2} & \frac{2I_b}{L_b} & \frac{6I_b}{L_b^2} & \frac{4I_b}{L_b} \end{bmatrix} \tag{17.40}$$

EXAMPLE 17.2

Determine the unknown nodal displacements and forces in the beam shown in Fig. 17.11. The beam is of uniform section throughout.

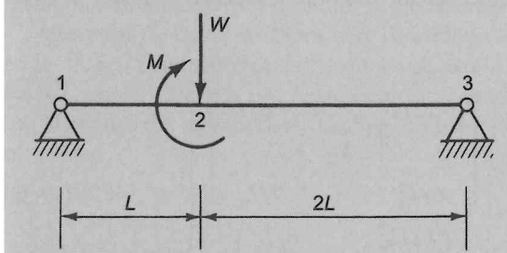

FIGURE 17.11
Beam of Ex. 17.2.

The beam may be idealized into two beam-elements, 1–2 and 2–3. From Fig. 17.11 we see that $v_1 = v_3 = 0$, $F_{y,2} = -W$, $M_2 = +M$. Therefore, eliminating rows and columns corresponding to zero displacements from Eq. (17.40), we obtain

$$\begin{Bmatrix} F_{y,2} = -W \\ M_2 = M \\ M_1 = 0 \\ M_3 = 0 \end{Bmatrix} = EI \begin{bmatrix} 27/2L^3 & 9/2L^2 & 6/L^2 & -3/2L^2 \\ 9/2L^2 & 6/L & 2/L & 1/L \\ 6/L^2 & 2/L & 4/L & 0 \\ -3/2L^2 & 1/L & 0 & 2/L \end{bmatrix} \begin{Bmatrix} v_2 \\ \theta_2 \\ \theta_1 \\ \theta_3 \end{Bmatrix} \tag{i}$$

Equation (i) may be written such that the elements of $[K]$ are pure numbers

$$\begin{Bmatrix} F_{y,2} = -W \\ M_2/L = M/L \\ M_1/L = 0 \\ M_3/L = 0 \end{Bmatrix} = \frac{EI}{2L^3} \begin{bmatrix} 27 & 9 & 12 & -3 \\ 9 & 12 & 4 & 2 \\ 12 & 4 & 8 & 0 \\ -3 & 2 & 0 & 4 \end{bmatrix} \begin{Bmatrix} v_2 \\ \theta_2 L \\ \theta_1 L \\ \theta_3 l \end{Bmatrix} \tag{ii}$$

Expanding Eq. (ii) by matrix multiplication we have

$$\begin{Bmatrix} -W \\ M/L \end{Bmatrix} = \frac{EI}{2L^3} \left(\begin{bmatrix} 27 & 9 \\ 9 & 12 \end{bmatrix} \begin{Bmatrix} v_2 \\ \theta_2 L \end{Bmatrix} + \begin{bmatrix} 12 & -3 \\ 4 & 2 \end{bmatrix} \begin{Bmatrix} \theta_1 L \\ \theta_3 L \end{Bmatrix} \right) \tag{iii}$$

and

$$\begin{Bmatrix} 0 \\ 0 \end{Bmatrix} = \frac{EI}{2L^3} \left(\begin{bmatrix} 12 & 4 \\ -3 & 2 \end{bmatrix} \begin{Bmatrix} v_2 \\ \theta_2 L \end{Bmatrix} + \begin{bmatrix} 8 & 0 \\ 0 & 4 \end{bmatrix} \begin{Bmatrix} \theta_1 L \\ \theta_3 L \end{Bmatrix} \right) \tag{iv}$$

Equation (iv) gives

$$\begin{Bmatrix} \theta_1 L \\ \theta_3 L \end{Bmatrix} = \begin{bmatrix} -\frac{3}{2} & -\frac{1}{2} \\ -\frac{3}{4} & -\frac{1}{2} \end{bmatrix} \begin{Bmatrix} v_2 \\ \theta_2 L \end{Bmatrix} \tag{v}$$

Substituting Eq. (v) in Eq. (iii) we obtain

$$\begin{Bmatrix} v_2 \\ \theta_2 L \end{Bmatrix} = \frac{L^3}{9EI} \begin{bmatrix} -4 & -2 \\ -2 & 3 \end{bmatrix} \begin{Bmatrix} -W \\ M/L \end{Bmatrix} \tag{vi}$$

from which the unknown displacements at node 2 are

$$v_2 = -\frac{4}{9}\frac{WL^3}{EI} - \frac{2}{9}\frac{ML^2}{EI}$$

$$\theta_2 = \frac{2}{9}\frac{WL^2}{EI} + \frac{1}{3}\frac{ML}{EI}$$

In addition, from Eq. (v) we find that

$$\theta_1 = \frac{5}{9}\frac{WL^2}{EI} + \frac{1}{6}\frac{ML}{EI}$$

$$\theta_3 = -\frac{4}{9}\frac{WL^2}{EI} - \frac{1}{3}\frac{ML}{EI}$$

It should be noted that the solution has been obtained by inverting two 2×2 matrices rather than the 4×4 matrix of Eq. (ii). This simplification has been brought about by the fact that $M_1 = M_3 = 0$.

The internal shear forces and bending moments can now be found using Eq. (17.37). For the beam-element 1–2 we have

$$S_{y,12} = EI\left(\frac{12}{L^3}v_1 - \frac{6}{L^2}\theta_1 - \frac{12}{L^3}v_2 - \frac{6}{L^2}\theta_2\right)$$

or

$$S_{y,12} = \frac{2}{3}W - \frac{1}{3}\frac{M}{L}$$

and

$$M_{12} = EI\left[\left(\frac{12}{L^3}x - \frac{6}{L^2}\right)v_1 + \left(-\frac{6}{L^2}x + \frac{4}{L}\right)\theta_1 + \left(-\frac{12}{L^3}x + \frac{6}{L^2}\right)v_2 + \left(-\frac{6}{L^2}x + \frac{2}{L}\right)\theta_2\right]$$

which reduces to

$$M_{12} = \left(\frac{2}{3}W - \frac{1}{3}\frac{M}{L}\right)x$$

7.3 Finite element method for continuum structures

n the previous sections we have discussed the matrix method of solution of structures composed of ele-ients connected only at nodal points. For skeletal structures consisting of arrangements of beams these odal points fall naturally at joints and at positions of concentrated loading. Continuum structures, such s flat plates, aircraft skins, shells, etc., do not possess such natural subdivisions and must therefore be rtificially idealized into a number of elements before matrix methods can be used. These *finite elements*, s they are known, may be two- or three-dimensional but the most commonly used are two-dimensional iangular and quadrilateral shaped elements. The idealization may be carried out in any number of dif-rent ways depending on such factors as the type of problem, the accuracy of the solution required and ie time and money available. For example, a *coarse* idealization involving a small number of large ele-ients would provide a comparatively rapid but very approximate solution while a *fine* idealization of nall elements would produce more accurate results but would take longer and consequently cost more. requently, *graded meshes* are used in which small elements are placed in regions where high stress con-ntrations are expected, e.g. around cut-outs and loading points. The principle is illustrated in ig. 17.12 where a graded system of triangular elements is used to examine the stress concentration ound a circular hole in a flat plate.

Although the elements are connected at an infinite number of points around their boundaries it is ssumed that they are only interconnected at their corners or nodes. Thus, compatibility of displace-ient is only ensured at the nodal points. However, in the finite element method a displacement pat-rn is chosen for each element which may satisfy some, if not all, of the compatibility requirements ong the sides of adjacent elements.

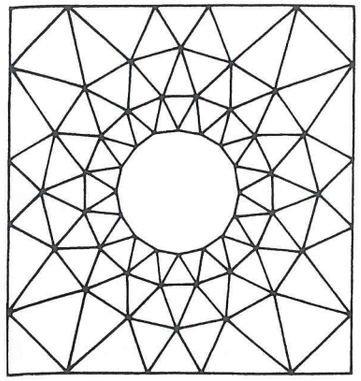

FIGURE 17.12
Finite element idealization of a flat plate with a central hole.

Since we are employing matrix methods of solution we are concerned initially with the determination of nodal forces and displacements. Thus, the system of loads on the structure must be replaced by an equivalent system of nodal forces. Where these loads are concentrated the elements are chosen such that a node occurs at the point of application of the load. In the case of distributed loads, equivalent nodal concentrated loads must be calculated.

The solution procedure is identical in outline to that described in the previous sections for skeletal structures; the differences lie in the idealization of the structure into finite elements and the calculation of the stiffness matrix for each element. The latter procedure, which in general terms is applicable to all finite elements, may be specified in a number of distinct steps. We shall illustrate the method by establishing the stiffness matrix for the simple one-dimensional beam-element of Fig. 17.6 for which we have already derived the stiffness matrix using slope–deflection.

Stiffness matrix for a beam-element

The first step is to choose a suitable coordinate and node numbering system for the element and define its nodal displacement vector $\{\delta^e\}$ and nodal load vector $\{F^e\}$. Use is made here of the superscript e to denote element vectors since, in general, a finite element possesses more than two nodes. Again we are not concerned with axial or shear displacements so that for the beam-element of Fig. 17.6 we have

$$\{\delta^e\} = \begin{Bmatrix} v_i \\ \theta_i \\ v_j \\ \theta_j \end{Bmatrix} \quad \{F^e\} = \begin{Bmatrix} F_{y,i} \\ M_i \\ F_{y,j} \\ M_j \end{Bmatrix}$$

Since each of these vectors contains four terms the element stiffness matrix $[K^e]$ will be of order 4×4.

In the second step we select a displacement function which uniquely defines the displacement of all points in the beam-element in terms of the nodal displacements. This displacement function may be taken as a polynomial which must include four arbitrary constants corresponding to the four nodal degrees of freedom of the element. Thus

$$v(x) = \alpha_1 + \alpha_2 x + \alpha_3 x^2 + \alpha_4 x^3 \tag{17.41}$$

Equation (17.41) is of the same form as that derived from elementary bending theory for a beam

$$\{v(x)\} = \begin{bmatrix} 1 & x & x^2 & x^3 \end{bmatrix} \begin{Bmatrix} \alpha_1 \\ \alpha_2 \\ \alpha_3 \\ \alpha_4 \end{Bmatrix}$$

or in abbreviated form as

$$\{v(x)\} = [f(x)]\{\alpha\} \tag{17.42}$$

The rotation θ at any section of the beam-element is given by $\partial v/\partial x$; therefore

$$\theta = \alpha_2 + 2\alpha_3 x + 3\alpha_4 x^2 \tag{17.43}$$

From Eqs (17.41) and (17.43) we can write down expressions for the nodal displacements v_i, θ_i and v_j, θ_j at $x = 0$ and $x = L$, respectively. Hence

$$\left.\begin{aligned} v_i &= \alpha_1 \\ \theta_i &= \alpha_2 \\ v_j &= \alpha_1 + \alpha_2 L + \alpha_3 L^2 + \alpha_4 L^3 \\ \theta_j &= \alpha_2 + 2\alpha_3 L + 3\alpha_4 L^2 \end{aligned}\right\} \tag{17.44}$$

Writing Eq. (17.44) in matrix form gives

$$\begin{Bmatrix} v_i \\ \theta_i \\ v_j \\ \theta_j \end{Bmatrix} = \begin{bmatrix} 1 & 0 & 0 & 0 \\ 0 & 1 & 0 & 0 \\ 1 & L & L^2 & L^3 \\ 0 & 1 & 2L & 3L^2 \end{bmatrix} \begin{Bmatrix} \alpha_1 \\ \alpha_2 \\ \alpha_3 \\ \alpha_4 \end{Bmatrix} \tag{17.45}$$

or

$$\{\delta^e\} = [A]\{\alpha\} \tag{17.46}$$

The third step follows directly from Eqs (17.45) and (17.42) in that we express the displacement at any point in the beam-element in terms of the nodal displacements. Using Eq. (17.46) we obtain

$$\{\alpha\} = [A^{-1}]\{\delta^e\} \tag{17.47}$$

Substituting in Eq. (17.42) gives

$$\{v(x)\} = [f(x)][A^{-1}]\{\delta^e\} \tag{17.48}$$

where $[A^{-1}]$ is obtained by inverting $[A]$ in Eq. (17.45) and may be shown to be given by

$$[A^{-1}] = \begin{bmatrix} 1 & 0 & 0 & 0 \\ 0 & 1 & 0 & 0 \\ -3/L^2 & -2/L & 3/L^2 & -1/L \\ 2/L^3 & 1/L^2 & -2/L^3 & 1/L^2 \end{bmatrix} \tag{17.49}$$

In step four we relate the strain $\{\varepsilon(x)\}$ at any point x in the element to the displacement $\{v(x)\}$ and hence to the nodal displacements $\{\delta^e\}$. Since we are concerned here with bending deformations only we may represent the strain by the curvature $\partial^2 v/\partial x^2$. Hence from Eq. (17.41)

$$\frac{\partial^2 v}{\partial x^2} = 2\alpha_3 + 6\alpha_4 x \tag{17.50}$$

or in matrix form

$$\{\varepsilon\} = \begin{bmatrix} 0 & 0 & 2 & 6x \end{bmatrix} \begin{Bmatrix} \alpha_1 \\ \alpha_2 \\ \alpha_3 \\ \alpha_4 \end{Bmatrix} \tag{17.51}$$

which we write as

$$\{\varepsilon\} = [C]\{\alpha\} \tag{17.52}$$

Substituting for $\{\alpha\}$ in Eq. (17.52) from Eq. (17.47) we have

$$\{\varepsilon\} = [C][A^{-1}]\{\delta^e\} \tag{17.53}$$

Step five relates the internal stresses in the element to the strain $\{\varepsilon\}$ and hence, using Eq. (17.53), to the nodal displacements $\{\delta^e\}$. In our beam-element the stress distribution at any section depends entirely on the value of the bending moment M at that section. Thus we may represent a 'state of stress' $\{\sigma\}$ at any section by the bending moment M, which, from simple beam theory, is given by

$$M = -EI\frac{\partial^2 v}{\partial x^2}$$

or

$$\{\sigma\} = [EI]\{\varepsilon\} \tag{17.54}$$

which we write as

$$\{\sigma\} = [D]\{\varepsilon\} \tag{17.55}$$

The matrix $[D]$ in Eq. (17.55) is the 'elasticity' matrix relating 'stress' and 'strain'. In this case $[D]$ consists of a single term, the flexural rigidity EI of the beam. Generally, however, $[D]$ is of a higher order. If we now substitute for $\{\varepsilon\}$ in Eq. (17.55) from Eq. (17.53) we obtain the 'stress' in terms of the nodal displacements, i.e.

$$\{\sigma\} = [D][C][A^{-1}]\{\delta^e\} \tag{17.56}$$

The element stiffness matrix is finally obtained in step six in which we replace the internal 'stresses' $\{\sigma\}$ by a statically equivalent nodal load system $\{F^e\}$, thereby relating nodal loads to nodal displacements (from Eq. (17.56)) and defining the element stiffness matrix $[K^e]$. This is achieved by employing the principle of the stationary value of the total potential energy of the beam (see Section 15.3) which comprises the internal strain energy U and the potential energy V of the nodal loads. Thus

$$U + V = \frac{1}{2}\int_{\text{vol}} \{\varepsilon\}^{\mathrm{T}}\{\sigma\}\,\mathrm{d(vol)} - \{\delta^e\}^{\mathrm{T}}\{F^e\} \tag{17.57}$$

Substituting in Eq. (17.57) for $\{\varepsilon\}$ from Eq. (17.53) and $\{\sigma\}$ from Eq. (17.56) we have

$$U + V = \frac{1}{2}\int_{\text{vol}} \{\delta^e\}^{\mathrm{T}}[A^{-1}]^{\mathrm{T}}[C]^{\mathrm{T}}[D][C][A^{-1}]\{\delta^e\}\mathrm{d(vol)} - \{\delta^e\}^{\mathrm{T}}\{F^e\} \tag{17.58}$$

The total potential energy of the beam has a stationary value with respect to the nodal displacements $\{\delta^e\}^{\mathrm{T}}$; hence, from Eq. (17.58)

$$\frac{\partial(U+V)}{\partial\{\delta^e\}^{\mathrm{T}}} = \int_{\text{vol}} [A^{-1}]^{\mathrm{T}}[C]^{\mathrm{T}}[D][C][A^{-1}]\{\delta^e\}\,\mathrm{d(vol)} - \{F^e\} = 0 \tag{17.59}$$

hence

$$\{F^e\} = \left[\int_{\text{vol}} [C]^T[A^{-1}]^T[D][C][A^{-1}]\,\mathrm{d(vol)}\right]\{\delta^e\} \tag{17.60}$$

writing $[C][A^{-1}]$ as $[B]$ we obtain

$$\{F^e\} = \left[\int_{\text{vol}} [B]^T[D][B]\,\mathrm{d(vol)}\right]\{\delta^e\} \tag{17.61}$$

om which the element stiffness matrix is clearly

$$\{K^e\} = \left[\int_{\text{vol}} [B]^T[D][B]\,\mathrm{d(vol)}\right] \tag{17.62}$$

From Eqs (17.49) and (17.51) we have

$$[B] = [C][A^{-1}] = \begin{bmatrix}0 & 0 & 2 & 6x\end{bmatrix}\begin{bmatrix}1 & 0 & 0 & 0\\ 0 & 1 & 0 & 0\\ -3/L^2 & -2/L & 3/L^2 & -1/L\\ 2/L^3 & 1/L^2 & -2/L^3 & 1/L^2\end{bmatrix}$$

$$[B]^T = \begin{bmatrix}-\frac{6}{L^2}+\frac{12x}{L^3}\\ -\frac{4}{L}+\frac{6x}{L^2}\\ \frac{6}{L^2}-\frac{12x}{L^3}\\ -\frac{2}{L}+\frac{6x}{L^2}\end{bmatrix} \tag{17.63}$$

Hence

$$[K^e] = \int_0^L \begin{bmatrix}-\frac{6}{L^2}+\frac{12x}{L^3}\\ -\frac{4}{L}+\frac{6x}{L^2}\\ \frac{6}{L^2}-\frac{12x}{L^3}\\ -\frac{2}{L}+\frac{6x}{L^2}\end{bmatrix}[EI]\begin{bmatrix}-\frac{6}{L^2}+\frac{12x}{L^3} & -\frac{4}{L}+\frac{6x}{L^2} & \frac{6}{L^2}-\frac{12x}{L^3} & -\frac{2}{L}+\frac{6x}{L^2}\end{bmatrix}\mathrm{d}x$$

hich gives

$$[K^e] = \frac{EI}{L^3}\begin{bmatrix}12 & -6L & -12 & -6L\\ -6L & 4L^2 & 6L & 2L^2\\ -12 & 6L & 12 & 6L\\ -6L & 2L^2 & 6L & 4L^2\end{bmatrix} \tag{17.64}$$

Equation (17.64) is identical to the stiffness matrix (see Eq. (17.31)) for the uniform beam of Fig. 17.6.

Finally, in step seven, we relate the internal 'stresses', $\{\sigma\}$, in the element to the nodal displacements $\{\delta^e\}$. In fact, this has been achieved to some extent in Eq. (17.56), namely

$$\{\sigma\} = [D][C][A^{-1}]\{\delta^e\}$$

or, from the above

$$\{\sigma\} = [D][B]\{\delta^e\} \tag{17.65}$$

Equation (17.65) is usually written

$$\{\sigma\} = [H]\{\delta^e\} \tag{17.66}$$

in which $[H] = [D][B]$ is the stress–displacement matrix. For this particular beam-element $[D] = EI$ and $[B]$ is defined in Eq. (17.63). Thus

$$[H] = EI\left[-\frac{6}{L^2}+\frac{12}{L^3}x \quad -\frac{4}{L}+\frac{6}{L^2}x \quad \frac{6}{L^2}-\frac{12}{L^3}x \quad -\frac{2}{L}+\frac{6}{L^2}x\right] \tag{17.67}$$

Stiffness matrix for a triangular finite element

Triangular finite elements are used in the solution of plane stress and plane strain problems. Their advantage over other shaped elements lies in their ability to represent irregular shapes and boundaries with relative simplicity.

In the derivation of the stiffness matrix we shall adopt the step by step procedure of the previous example. Initially, therefore, we choose a suitable coordinate and node numbering system for the element and define its nodal displacement and nodal force vectors. Figure 17.13 shows a triangular element referred to axes Oxy and having nodes i, j and k lettered anticlockwise. It may be shown that the inverse of the $[A]$ matrix for a triangular element contains terms giving the actual area of the element; this area is positive if the above node lettering or numbering system is adopted. The element is to be used for plane elasticity problems and has therefore two degrees of freedom per node, giving a total of six degrees of freedom for the element, which will result in a 6×6 element stiffness matrix $[K^e]$. The nodal forces and displacements are shown and the complete displacement and force vectors are

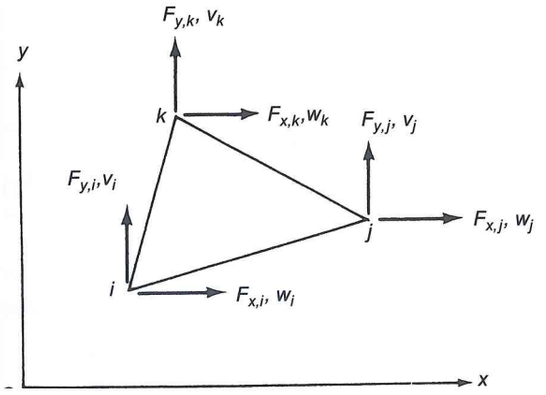

FIGURE 17.13
Triangular element for plane elasticity

$$\{\delta^e\} = \begin{Bmatrix} w_i \\ v_i \\ w_j \\ v_j \\ w_k \\ v_k \end{Bmatrix} \quad \{F^e\} = \begin{Bmatrix} F_{x,i} \\ F_{y,i} \\ F_{x,j} \\ F_{y,j} \\ F_{x,k} \\ F_{y,k} \end{Bmatrix} \tag{17.68}$$

We now select a displacement function which must satisfy the boundary conditions of the element, . the condition that each node possesses two degrees of freedom. Generally, for computational pur- ses, a polynomial is preferable to, say, a trigonometric series since the terms in a polynomial can be culated much more rapidly by a digital computer. Furthermore, the total number of degrees of free- m is six, so that only six coefficients in the polynomial can be obtained. Suppose that the displace- ent function is

$$\left.\begin{aligned} w(x,y) &= \alpha_1 + \alpha_2 x + \alpha_3 y \\ v(x,y) &= \alpha_4 + \alpha_5 x + \alpha_6 y \end{aligned}\right\} \tag{17.69}$$

The constant terms, α_1 and α_4, are required to represent any in-plane rigid body motion, i.e. tion without strain, while the linear terms enable states of constant strain to be specified; . (17.69) ensures compatibility of displacement along the edges of adjacent elements. Writing . (17.69) in matrix form gives

$$\begin{Bmatrix} w(x,y) \\ v(x,y) \end{Bmatrix} = \begin{bmatrix} 1 & x & y & 0 & 0 & 0 \\ 0 & 0 & 0 & 1 & x & y \end{bmatrix} \begin{Bmatrix} \alpha_1 \\ \alpha_2 \\ \alpha_3 \\ \alpha_4 \\ \alpha_5 \\ \alpha_6 \end{Bmatrix} \tag{17.70}$$

Comparing Eq. (17.70) with Eq. (17.42) we see that it is of the form

$$\begin{Bmatrix} w(x,y) \\ v(x,y) \end{Bmatrix} = [f(x,y)]\{\alpha\} \tag{17.71}$$

Substituting values of displacement and coordinates at each node in Eq. (17.71) we have, for node i

$$\begin{Bmatrix} w_i \\ v_i \end{Bmatrix} = \begin{bmatrix} 1 & x_i & y_i & 0 & 0 & 0 \\ 0 & 0 & 0 & 1 & x_i & y_i \end{bmatrix} \{\alpha\}$$

Similar expressions are obtained for nodes j and k so that for the complete element we obtain

$$\begin{Bmatrix} w_i \\ v_i \\ w_j \\ v_j \\ w_k \\ v_k \end{Bmatrix} = \begin{bmatrix} 1 & x_i & y_i & 0 & 0 & 0 \\ 0 & 0 & 0 & 1 & x_i & y_i \\ 1 & x_j & x_j & 0 & 0 & 0 \\ 0 & 0 & 0 & 1 & x_j & y_j \\ 1 & x_k & y_k & 0 & 0 & 0 \\ 0 & 0 & 0 & 1 & x_k & y_k \end{bmatrix} \begin{Bmatrix} \alpha_1 \\ \alpha_2 \\ \alpha_3 \\ \alpha_4 \\ \alpha_5 \\ \alpha_6 \end{Bmatrix} \tag{17.72}$$

From Eq. (17.68) and by comparison with Eqs (17.45) and (17.46) we see that Eq. (17.72) takes form

$$\{\delta^e\} = [A]\{\alpha\}$$

Hence (step 3) we obtain

$$\{\alpha\} = [A^{-1}]\{\delta^e\} \text{ (compare with Eq. (17.47))}$$

The inversion of $[A]$, defined in Eq. (17.72), may be achieved algebraically as illustrated in Ex. 17.3. Alternatively, the inversion may be carried out numerically for a particular element by computer. Substituting for $\{\alpha\}$ from the above into Eq. (17.71) gives

$$\begin{Bmatrix} w(x,y) \\ v(x,y) \end{Bmatrix} = [f(x,y)][A^{-1}]\{\delta^e\} \text{ (compare with Eq. (17.48))} \tag{17.73}$$

The strains in the element are

$$\{\varepsilon\} = \begin{Bmatrix} \varepsilon_x \\ \varepsilon_y \\ \gamma_{xy} \end{Bmatrix} \tag{17.74}$$

Direct and shear strains may be defined in the form

$$\varepsilon_x = \frac{\partial w}{\partial x} \quad \varepsilon_y = \frac{\partial v}{\partial y} \quad \gamma_{xy} = \frac{\partial w}{\partial y} + \frac{\partial v}{\partial x} \tag{17.75}$$

Substituting for w and v in Eq. (17.75) from Eq. (17.69) gives

$$\begin{aligned} \varepsilon_x &= \alpha_2 \\ \varepsilon_y &= \alpha_6 \\ \gamma_{xy} &= \alpha_3 + \alpha_5 \end{aligned}$$

or in matrix form

$$\{\varepsilon\} = \begin{bmatrix} 0 & 1 & 0 & 0 & 0 & 0 \\ 0 & 0 & 0 & 0 & 0 & 1 \\ 0 & 0 & 1 & 0 & 1 & 0 \end{bmatrix} \begin{Bmatrix} \alpha_1 \\ \alpha_2 \\ \alpha_3 \\ \alpha_4 \\ \alpha_5 \\ \alpha_6 \end{Bmatrix} \tag{17.76}$$

which is of the form

$$\{\varepsilon\} = [C]\{\alpha\} \text{ (see Eps (17.51) and (17.52))}$$

Substituting for $\{\alpha\}$ $(=[A^{-1}]\{\delta^e\})$ we obtain

$$\{\varepsilon\} = [C][A^{-1}]\{\delta^e\} \text{ (compare with Eq. (17.53))}$$

or

$$\{\varepsilon\} = [B]\{\delta^e\} \text{ (see Eq. (17.63))}$$

where $[C]$ is defined in Eq. (17.76).

In step five we relate the internal stresses $\{\sigma\}$ to the strain $\{\varepsilon\}$ and hence, using step four, to the nodal displacements $\{\delta^e\}$. For plane stress problems

$$\{\sigma\} = \begin{Bmatrix} \sigma_x \\ \sigma_y \\ \tau_{xy} \end{Bmatrix} \tag{17.77}$$

d

$$\left.\begin{aligned}\varepsilon_x &= \frac{\sigma_x}{E} - \frac{v\sigma_x}{E}\\ \varepsilon_y &= \frac{\sigma_y}{E} - \frac{v\sigma_x}{E}\\ \gamma_{xy} &= \frac{\tau_{xy}}{G} = \frac{2(1+v)}{E}\tau_{xy}\end{aligned}\right\} \text{(see Chapter 7)}$$

Thus, in matrix form

$$\{\varepsilon\} = \begin{Bmatrix}\varepsilon_x\\ \varepsilon_y\\ \gamma_{xy}\end{Bmatrix} = \frac{1}{E}\begin{bmatrix}1 & -v & 0\\ -v & 1 & 0\\ 0 & 0 & 2(1+v)\end{bmatrix}\begin{Bmatrix}\sigma_x\\ \sigma_y\\ \tau_{xy}\end{Bmatrix} \tag{17.78}$$

It may be shown that

$$\{\sigma\} = \begin{Bmatrix}\sigma_x\\ \sigma_y\\ \gamma_{xy}\end{Bmatrix} = \frac{E}{1-v^2}\begin{bmatrix}1 & v & 0\\ v & 1 & 0\\ 0 & 0 & \frac{1}{2}(1-v)\end{bmatrix}\begin{Bmatrix}\varepsilon_x\\ \varepsilon_y\\ \gamma_{xy}\end{Bmatrix} \tag{17.79}$$

ich has the form of Eq. (17.55), i.e.

$$\{\sigma\} = [D]\{\varepsilon\}$$

Substituting for $\{\varepsilon\}$ in terms of the nodal displacements $\{\delta^e\}$ we obtain

$$\{\sigma\} = [D][B]\{\delta^e\} \text{ (see Eq. (17.56))}$$

In the case of plane strain the elasticity matrix $[D]$ takes a different form to that defined in . (17.79). For this type of problem

$$\varepsilon_x = \frac{\sigma_x}{E} - \frac{v\sigma_y}{E} - \frac{v\sigma_z}{E}$$

$$\varepsilon_y = \frac{\sigma_y}{E} - \frac{v\sigma_x}{E} - \frac{v\sigma_z}{E}$$

$$\varepsilon_z = \frac{\sigma_z}{E} - \frac{v\sigma_x}{E} - \frac{v\sigma_y}{E} = 0$$

$$\gamma_{xy} = \frac{\tau_{xy}}{G} = \frac{2(1+v)}{E}\tau_{xy}$$

Eliminating σ_z and solving for σ_x, σ_y and τ_{xy} gives

$$\{\sigma\} = \begin{Bmatrix}\sigma_x\\ \sigma_y\\ \tau_{xy}\end{Bmatrix} = \frac{E(1-v)}{(1-v)(1-2v)}\begin{bmatrix}1 & \frac{v}{1-v} & 0\\ \frac{v}{1-v} & 1 & 0\\ 0 & 0 & \frac{(1-2v)}{2(1-v)}\end{bmatrix}\begin{Bmatrix}\varepsilon_x\\ \varepsilon_y\\ \gamma_{xy}\end{Bmatrix} \tag{17.80}$$

which again takes the form

$$\{\sigma\} = [D]\{\varepsilon\}$$

Step six, in which the internal stresses $\{\sigma\}$ are replaced by the statically equivalent nodal forces $\{F^e\}$ proceeds, in an identical manner to that described for the beam-element. Thus

$$[F^e] = \left[\int_{\text{vol}} [B]^{\mathrm{T}}[D][B]\,\mathrm{d(vol)}\right]\{\delta^e\}$$

as in Eq. (17.61), whence

$$[K^e] = \left[\int_{\text{vol}} [B]^{\mathrm{T}}[D][B]\,\mathrm{d(vol)}\right]$$

In this expression $[B] = [C][A^{-1}]$ where $[A]$ is defined in Eq. (17.72) and $[C]$ in Eq. (17.76). The elasticity matrix $[D]$ is defined in Eq. (17.79) for plane stress problems or in Eq. (17.80) for plane strain problems. We note that the $[C]$, $[A]$ (therefore $[B]$) and $[D]$ matrices contain only constant terms and may therefore be taken outside the integration in the expression for $[K^e]$, leaving only $\int \mathrm{d(vol)}$ which is simply the area, A, of the triangle times its thickness t. Thus

$$[K^e] = [[B]^{\mathrm{T}}[D][B]At] \tag{17.81}$$

Finally the element stresses follow from Eq. (17.66), i.e.

$$\{\sigma\} = [H]\{\delta^e\}$$

where $[H] = [D][B]$ and $[D]$ and $[B]$ have previously been defined. It is usually found convenient to plot the stresses at the centroid of the element.

Of all the finite elements in use the triangular element is probably the most versatile. It may be used to solve a variety of problems ranging from two-dimensional flat plate structures to three-dimensional folded plates and shells. For three-dimensional applications the element stiffness matrix $[K^e]$ is transformed from an in-plane xy coordinate system to a three-dimensional system of global coordinates by the use of a transformation matrix similar to those developed for the matrix analysis of skeletal structures. In addition to the above, triangular elements may be adapted for use in plate flexure problems and for the analysis of bodies of revolution.

EXAMPLE 17.3

A constant strain triangular element has corners 1(0, 0), 2(4, 0) and 3(2, 2) referred to a Cartesian Oxy axes system and is 1 unit thick. If the elasticity matrix $[D]$ has elements $D_{11} = D_{22} = a$, $D_{12} = D_{21} = b$, $D_{13} = D_{23} = D_{31} = D_{32} = 0$ and $D_{33} = c$, derive the stiffness matrix for the element.

From Eq. (17.69)

$$w_1 = \alpha_1 + \alpha_2(0) + \alpha_3(0)$$

i.e.

$$\left.\begin{aligned}w_1 &= \alpha_1\\ w_2 &= \alpha_1 + \alpha_2(4) + \alpha_3(0)\end{aligned}\right\} \tag{i}$$

i.e.

$$w_2 = \alpha_1 + 4\alpha_2 \tag{ii}$$

e.

$$w_3 = \alpha_1 + 2\alpha_2 + 2\alpha_3 \tag{iii}$$

From Eq. (i)

$$\alpha_1 = w_1 \tag{iv}$$

nd from Eqs (ii) and (iv)

$$\alpha_2 = \frac{w_2 - w_1}{4} \tag{v}$$

Then, from Eqs (iii)–(v)

$$\alpha_3 = \frac{2w_3 - w_1 - w_2}{4} \tag{vi}$$

Substituting for α_1, α_2 and α_3 in the first of Eq. (17.69) gives

$$w = w_1 + \left(\frac{w_2 - w_1}{4}\right)x + \left(\frac{2w_3 - w_1 - w_2}{4}\right)y$$

r

$$w = \left(1 - \frac{x}{4} - \frac{y}{4}\right)w_1 + \left(\frac{x}{4} - \frac{y}{4}\right)w_2 + \frac{y}{2}w_3 \tag{vii}$$

Similarly

$$v = \left(1 - \frac{x}{4} - \frac{y}{4}\right)v_1 + \left(\frac{x}{4} - \frac{y}{4}\right)v_2 + \frac{y}{2}v_3 \tag{viii}$$

Now from Eq. (17.75)

$$\varepsilon_x = \frac{\partial w}{\partial x} = -\frac{w_1}{4} + \frac{w_2}{4}$$

$$\varepsilon_y = \frac{\partial v}{\partial y} = -\frac{v_1}{4} - \frac{v_2}{4} + \frac{v_3}{2}$$

nd

$$\gamma_{xy} = \frac{\partial w}{\partial y} + \frac{\partial v}{\partial x} = -\frac{w_1}{4} - \frac{w_2}{4} - \frac{v_1}{4} + \frac{v_2}{4}$$

Hence

$$[B]\{\delta^e\} = \begin{bmatrix} \dfrac{\partial w}{\partial x} \\ \dfrac{\partial v}{\partial y} \\ \dfrac{\partial w}{\partial y} + \dfrac{\partial v}{\partial x} \end{bmatrix} = \frac{1}{4}\begin{bmatrix} -1 & 0 & 1 & 0 & 0 & 0 \\ 0 & -1 & 0 & -1 & 0 & 2 \\ -1 & -1 & -1 & 1 & 2 & 0 \end{bmatrix}\begin{Bmatrix} w_1 \\ v_1 \\ w_2 \\ v_2 \\ w_3 \\ v_3 \end{Bmatrix} \tag{ix}$$

Also

$$[D] = \begin{bmatrix} a & b & 0 \\ b & a & 0 \\ 0 & 0 & c \end{bmatrix}$$

Hence

$$[D][B] = \frac{1}{4}\begin{bmatrix} -a & -b & a & -b & 0 & 2b \\ -b & -a & b & -a & 0 & 2a \\ -c & -c & -c & c & 2c & 0 \end{bmatrix}$$

and

$$[B]^T[D][B] = \frac{1}{16}\begin{bmatrix} a+b & b+c & -a+c & b-c & -2c & -2b \\ b+c & a+c & -b+c & a-c & -2c & -2a \\ -a+c & -b+c & a+c & -b-c & -2c & 2b \\ b-c & a-c & -b-c & a+c & 2c & -2a \\ -2c & -2c & -2c & 2c & 4c & 0 \\ -2b & -2a & 2b & -2a & 0 & 4a \end{bmatrix}$$

Then, from Eq. (17.81)

$$[K^e] = \frac{1}{4}\begin{bmatrix} a+c & b+c & -a+c & b-c & -2c & -2b \\ b+c & a+c & -b+c & a-c & -2c & -2a \\ -a+c & -b+c & a+c & -b-c & -2c & 2b \\ b-c & a-c & -b-c & a+c & 2c & -2a \\ -2c & -2c & -2c & 2c & 4c & 0 \\ -2b & -2a & 2b & -2a & 0 & 4a \end{bmatrix}$$

Stiffness matrix for a quadrilateral element

Quadrilateral elements are frequently used in combination with triangular elements to build up particular geometrical shapes.

Figure 17.14 shows a quadrilateral element referred to axes O*xy* and having corner nodes, *i*, *j*, *k* and *l*; the nodal forces and displacements are also shown and the displacement and force vectors are

$$\{\delta^e\} = \begin{Bmatrix} w_i \\ v_i \\ w_j \\ v_j \\ w_k \\ v_k \\ w_l \\ v_l \end{Bmatrix} \quad \{F^e\} = \begin{Bmatrix} F_{x,i} \\ F_{y,i} \\ F_{x,j} \\ F_{y,j} \\ F_{x,k} \\ F_{y,k} \\ F_{x,l} \\ F_{y,l} \end{Bmatrix} \tag{17.82}$$

As in the case of the triangular element we select a displacement function which satisfies the total of eight degrees of freedom of the nodes of the element; again this displacement function will be in the

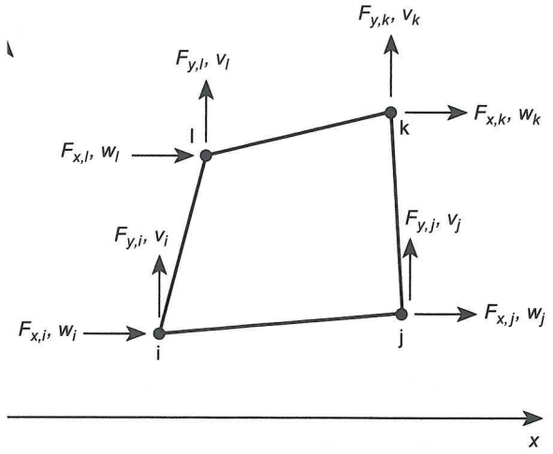

FIGURE 17.14
Quadrilateral element subjected to nodal in-plane forces and displacements.

$$\left.\begin{aligned} w(x,y) &= \alpha_1 + \alpha_2 x + \alpha_3 y + \alpha_4 xy \\ v(x,y) &= \alpha_5 + \alpha_6 x + \alpha_7 y + \alpha_8 xy \end{aligned}\right\} \tag{17.83}$$

The constant terms, α_1 and α_5, are required, as before, to represent the in-plane rigid body motion the element while the two pairs of linear terms enable states of constant strain to be represented oughout the element. Further, the inclusion of the xy terms results in both the $w(x,y)$ and $v(x,y)$ dis-cements having the same algebraic form so that the element behaves in exactly the same way in the x ection as it does in the y direction.

Writing Eq. (17.83) in matrix form gives

$$\begin{Bmatrix} w(x,y) \\ v(x,y) \end{Bmatrix} = \begin{bmatrix} 1 & x & y & xy & 0 & 0 & 0 & 0 \\ 0 & 0 & 0 & 0 & 1 & x & y & xy \end{bmatrix} \begin{Bmatrix} \alpha_1 \\ \alpha_2 \\ \alpha_3 \\ \alpha_4 \\ \alpha_5 \\ \alpha_6 \\ \alpha_7 \\ \alpha_8 \end{Bmatrix} \tag{17.84}$$

$$\begin{Bmatrix} w(x,y) \\ v(x,y) \end{Bmatrix} = [f(x,y)]\{\alpha\} \tag{17.85}$$

Now substituting the coordinates and values of displacement at each node we obtain

$$\begin{Bmatrix} w_i \\ v_i \\ w_j \\ v_j \\ w_k \\ v_k \\ w_l \\ \end{Bmatrix} = \begin{bmatrix} 1 & x_i & y_i & x_i y_i & 0 & 0 & 0 & 0 \\ 0 & 0 & 0 & 0 & 1 & x_i & y_i & x_i y_i \\ 1 & x_j & y_j & x_j y_j & 0 & 0 & 0 & 0 \\ 0 & 0 & 0 & 0 & 1 & x_j & y_j & x_j y_j \\ 1 & x_k & y_k & x_k y_k & 0 & 0 & 0 & 0 \\ 0 & 0 & 0 & 0 & 1 & x_k & y_k & x_k y_k \\ 1 & x_l & y_l & x_l y_l & 0 & 0 & 0 & 0 \end{bmatrix} \begin{Bmatrix} \alpha_1 \\ \alpha_2 \\ \alpha_3 \\ \alpha_4 \\ \alpha_5 \\ \alpha_6 \\ \alpha_7 \end{Bmatrix} \tag{17.86}$$

which is of the form

$$\{\delta^e\} = [A]\{\alpha\}$$

Then

$$\{\alpha\} = [A^{-1}]\{\delta^e\} \tag{17.87}$$

The inversion of $[A]$ is illustrated in Ex. 17.4 but, as in the case of the triangular element, is most easily carried out by means of a computer. The remaining analysis is identical to that for the triangular element except that the $\{\varepsilon\}-\{\alpha\}$ relationship (see Eq. (17.76)) becomes

$$\{\varepsilon\} = \begin{bmatrix} 0 & 1 & 0 & y & 0 & 0 & 0 & 0 \\ 0 & 0 & 0 & 0 & 0 & 0 & 1 & x \\ 0 & 0 & 1 & x & 0 & 1 & 0 & y \end{bmatrix} \begin{Bmatrix} \alpha_1 \\ \alpha_2 \\ \alpha_3 \\ \alpha_4 \\ \alpha_5 \\ \alpha_6 \\ \alpha_7 \\ \alpha_8 \end{Bmatrix} \tag{17.88}$$

EXAMPLE 17.4

A rectangular element used in a plane stress analysis has corners whose coordinates (in metres), referred to an Oxy axes system, are 1(−2, −1), 2(2, −1), 3(2, 1) and 4(−2, 1); the displacements (also in metres) of the corners were

$$\begin{aligned} w_1 &= 0.001 & w_2 &= 0.003 & w_3 &= -0.003 & w_4 &= 0 \\ v_1 &= -0.004 & v_2 &= -0.002 & v_3 &= 0.001 & v_4 &= 0.001 \end{aligned}$$

If Young's modulus $E = 200\ 000\ \text{N/mm}^2$ and Poisson's ratio $\upsilon = 0.3$, calculate the stresses at the centre of the element.

From the first of Eq. (17.83)

$$w_1 = \alpha_1 - 2\alpha_2 - \alpha_3 + 2\alpha_4 = 0.001 \tag{i}$$

$$w_2 = \alpha_1 + 2\alpha_2 - \alpha_3 - 2\alpha_4 = 0.003 \tag{ii}$$

$$w_3 = \alpha_1 + 2\alpha_2 + \alpha_3 + 2\alpha_4 = -0.003 \tag{iii}$$

$$w_4 = \alpha_1 - 2\alpha_2 + \alpha_3 - 2\alpha_4 = 0 \tag{iv}$$

Subtracting Eq. (ii) from Eq. (i)

$$\alpha_2 - \alpha_4 = 0.0005 \tag{v}$$

Now subtracting Eq. (iv) from Eq. (iii)

$$\alpha_2 + \alpha_4 = -0.00075 \tag{vi}$$

Then subtracting Eq. (vi) from Eq. (v)

$$\alpha_4 = -0.000625 \tag{vii}$$

whence, from either of Eqs (v) or (vi)

$$\alpha_2 = -0.000125 \tag{viii}$$

Adding Eqs (i) and (ii)

$$\alpha_1 - \alpha_3 = 0.002 \tag{ix}$$

Adding Eqs (iii) and (iv)

$$\alpha_1 + \alpha_3 = -0.0015 \tag{x}$$

Then adding Eqs (ix) and (x)

$$\alpha_1 = 0.00025 \tag{xi}$$

nd, from either of Eqs (ix) or (x)

$$\alpha_3 = -0.00175 \tag{xii}$$

The second of Eq. (17.83) is used to determine α_5, α_6, α_7 and α_8 in an identical manner to the bove. Thus

$$\alpha_5 = -0.001$$
$$\alpha_6 = 0.00025$$
$$\alpha_7 = 0.002$$
$$\alpha_8 = -0.00025$$

Now substituting for $\alpha_1, \alpha_2, \ldots, \alpha_8$ in Eq. (17.83)

$$w_i = 0.00025 - 0.000125x - 0.00175y - 0.000625xy$$

nd

$$v_i = -0.001 + 0.00025x + 0.002y - 0.00025xy$$

Then, from Eq. (17.75)

$$\varepsilon_x = \frac{\partial w}{\partial x} = -0.000125 - 0.000625y$$

$$\varepsilon_y = \frac{\partial v}{\partial y} = 0.002 - 0.00025x$$

$$\gamma_{xy} = \frac{\partial w}{\partial y} + \frac{\partial v}{\partial x} = -0.0015 - 0.000625x - 0.00025y$$

Therefore, at the centre of the element ($x = 0$, $y = 0$)

$$\varepsilon_x = -0.000125$$
$$\varepsilon_y = 0.002$$
$$\gamma_{xy} = -0.0015$$

› that, from Eq. (17.79)

$$\sigma_x = \frac{E}{1-\nu^2}(\varepsilon_x + \nu\varepsilon_y) = \frac{200\,000}{1-0.3^2}(-0.000125 + (0.3 \times 0.002))$$

i.e.

$$\sigma_x = 104.4 \text{ N/mm}^2$$

$$\sigma_y = \frac{E}{1-\nu^2}(\varepsilon_y + \nu\varepsilon_x) = \frac{200\,000}{1-0.3^2}(0.002 + (0.3 \times 0.000125))$$

i.e.

$$\sigma_y = 431.3 \text{ N/mm}^2$$

and

$$\tau_{xy} = \frac{E}{1-\nu^2} \times \frac{1}{2}(1-\nu)\gamma_{xy} = \frac{E}{2(1+\nu)}\gamma_{xy}$$

Thus

$$\tau_{xy} = \frac{200\,000}{2(1+0.3)} \times (-0.0015)$$

i.e.

$$\tau_{xy} = -11.5 \text{ N/mm}^2$$

The application of the finite element method to three-dimensional solid bodies is a straightforward extension of the analysis of two-dimensional structures. The basic three-dimensional elements are the tetrahedron and the rectangular prism, both shown in Fig. 17.15. The tetrahedron has four nodes each possessing three degrees of freedom, a total of 12 for the element, while the prism has 8 nodes and therefore a total of 24 degrees of freedom. Displacement functions for each element require polynomials in x, y and z; for the tetrahedron the displacement function is of the first degree with 12 constant coefficients, while that for the prism may be of a higher order to accommodate the 24 degrees of freedom. A development in the solution of three-dimensional problems has been the introduction of curvilinear coordinates. This enables the tetrahedron and prism to be distorted into arbitrary shapes that are better suited for fitting actual boundaries.

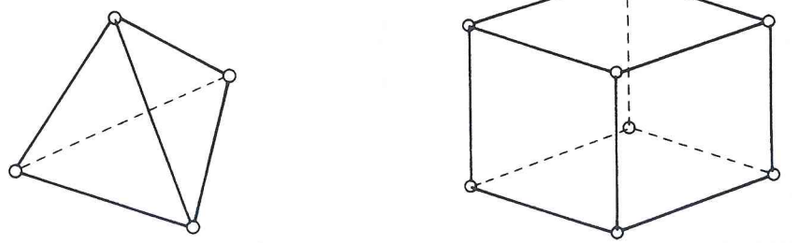

FIGURE 17.15

New elements and new applications of the finite element method are still being developed, some of which lie outside the field of structural analysis. These fields include soil mechanics, heat transfer, fluid and seepage flow, magnetism and electricity.

Problems

P.17.1 The truss shown in Fig. P.17.1 has members of cross sectional area 60 mm^2 and Young's modulus 210000 N/mm^2. Obtain the stiffness matrix for the truss and hence calculate the horizontal and vertical displacements at node 2.

Ans. 15.19 mm (to the right), 3.98 mm (downwards).

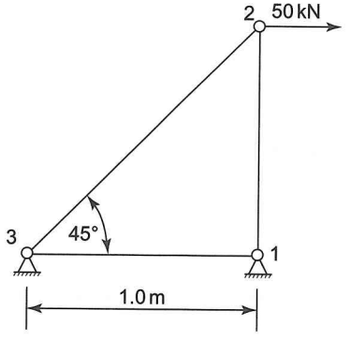

FIGURE P.17.1

P.17.2 Figure P.17.2 shows a square symmetrical pin-jointed truss 1234, pinned to rigid supports at 2 and 4 and loaded with a vertical load at 1. The axial rigidity *EA* is the same for all members.

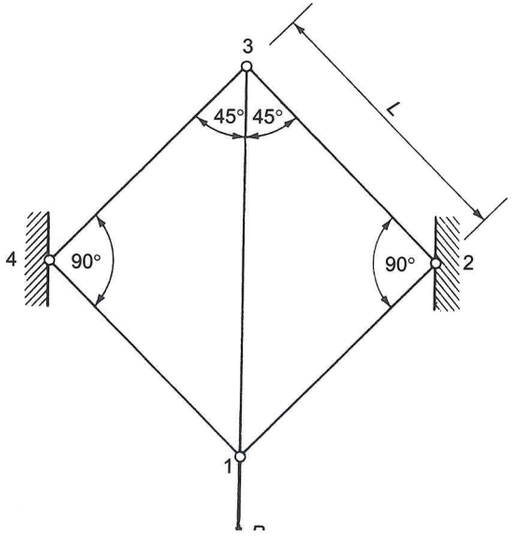

FIGURE P.17.2

Use the stiffness method to find the displacements at nodes 1 and 3 and hence solve for all the internal member forces and support reactions.

Ans. $v_1 = -PL/\sqrt{2}AE \quad v_3 = -0.293PL/AE \quad F_{12} = P/2 = F_{14}$
$F_{23} = -0.207P = F_{43} \quad F_{13} = 0.293P \quad F_{x,2} = -F_{x,4} = 0.207P$
$F_{y,2} = F_{y,4} = P/2.$

P.17.3 Use the stiffness method to find the ratio *H/P* for which the displacement of node 4 of the plane pin-jointed frame shown loaded in Fig. P.17.3 is zero, and for that case give the displacements of nodes 2 and 3.

All members have equal axial rigidity *EA*.

Ans. $H/P = 0.449 \quad v_2 = -4Pl/(9 + 2\sqrt{3})\,AE \quad v_3 = -6Pl/(9 + 2\sqrt{3})AE.$

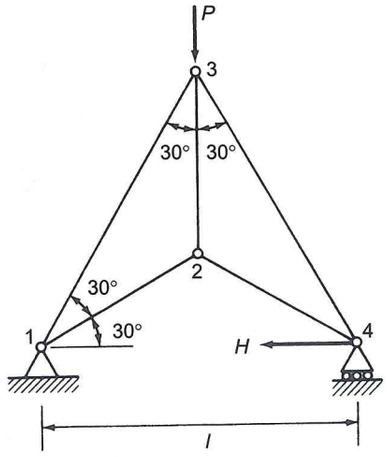

FIGURE P.17.3

P.17.4 Form the matrices required to solve completely the plane truss shown in Fig. P.17.4 and determine the force in member 24. All members have equal axial rigidity.

Ans. $F_{24} = 0.$

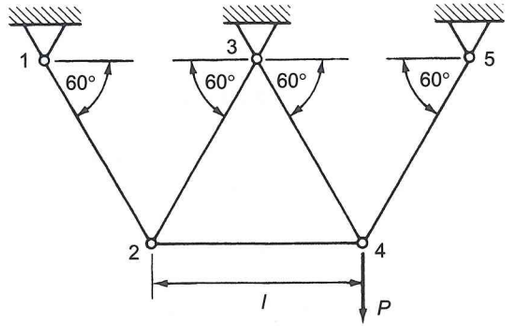

FIGURE P.17.4

P.17.5 The symmetrical plane rigid jointed frame 1234567, shown in Fig. P.17.5, is fixed to rigid supports at 1 and 5 and supported by rollers inclined at 45° to the horizontal at nodes 3 and 7. It

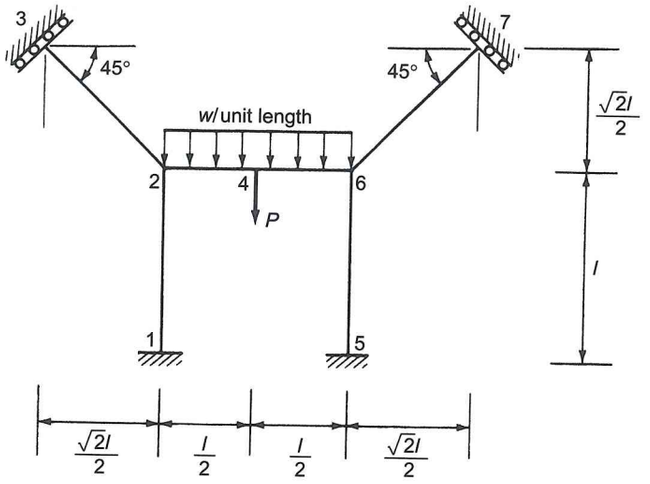

FIGURE P.17.5

span 26. Assuming the same flexural rigidity EI for all members, set up the stiffness equations which, when solved, give the nodal displacements of the frame.

Explain how the member forces can be obtained.

17.6 The frame shown in Fig. P.17.6 has the planes xz and yz as planes of symmetry. The nodal coordinates of one quarter of the frame are given in Table P.17.6(i).

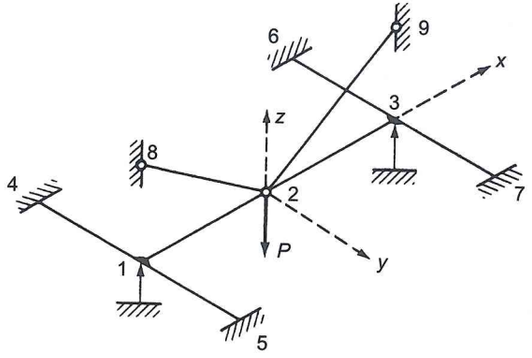

FIGURE P.17.6

In this structure the deformation of each member is due to a single effect, this being axial, bending or torsional. The mode of deformation of each member is given in Table P.17.6(ii), together with the relevant rigidity.

Use the *direct stiffness* method to find all the displacements and hence calculate the forces in all the members. For member 123 plot the shear force and bending moment diagrams.

Briefly outline the sequence of operations in a typical computer program suitable for linear frame analysis.

Ans. $F_{29} = F_{28} = \sqrt{2}P/6$ (tension) $M_3 = -M_1 = PL/9$ (hogging)
$M_2 = 2PL/9$ (sagging) $F_{y,3} = -F_{y,2} = P/3$.

Twisting moment in 37, $PL/18$ (anticlockwise)

Table P.17.6(i)

Node	x	y	z
2	0	0	0
3	L	0	0
7	L	$0.8L$	0
9	L	0	L

Table P.17.6(ii)

	Effect		
Member	Axial	Bending	Torsional
23	–	EI	–
37	–	–	$GJ = 0.8EI$
29	$EA = 6\sqrt{2}\frac{EI}{L^2}$	–	–

P.17.7 Given that the force–displacement (stiffness) relationship for the beam element shown in Fig. P.17.7(a) may be expressed in the following form:

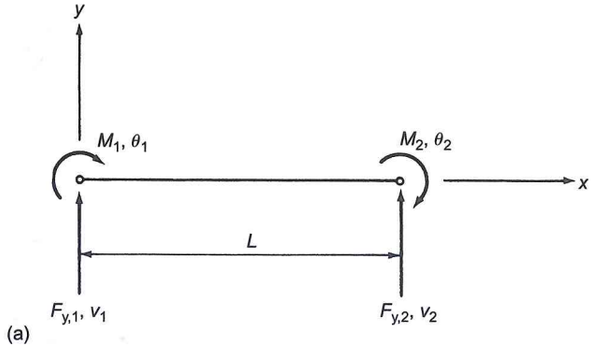

(a)

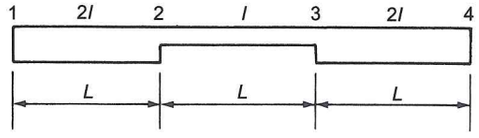

(b)

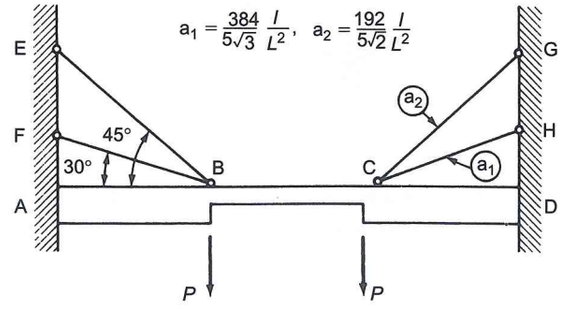

FIGURE P.17.7

$$\begin{Bmatrix} F_{y,1} \\ M_1/L \\ F_{y,2} \\ M_2/L \end{Bmatrix} = \frac{EI}{L^3} \begin{bmatrix} 12 & -6 & -12 & -6 \\ -6 & 4 & 6 & 2 \\ -12 & 6 & 12 & 6 \\ -6 & 2 & 6 & 4 \end{bmatrix} \begin{Bmatrix} v_1 \\ \theta_1 L \\ v_2 \\ \theta_2 L \end{Bmatrix}$$

obtain the force–displacement (stiffness) relationship for the variable section beam (Fig. P.17.7(b)), composed of elements 12, 23 and 34.

Such a beam is loaded and supported symmetrically as shown in Fig. P.17.7(c). Both ends are rigidly fixed and the ties FB, CH have a cross-sectional area a_1 and the ties EB, CG a cross-sectional area a_2. Calculate the deflections under the loads, the forces in the ties and all other information necessary for sketching the bending moment and shear force diagrams for the beam.

Neglect axial effects in the beam. The ties are made from the same material as the beam.

Ans. $v_B = v_C = -5PL^3/144EI \quad \theta_B = -\theta_C = PL^2/24EI \quad F_{BF} = 2P/3$
$F_{BE} = \sqrt{2}P/3 \; F_{y,A} = P/3 \quad M_A = -PL/4.$

17.8 The symmetrical rigid jointed grillage shown in Fig. P.17.8 is encastré at 6, 7, 8 and 9 and rests on simple supports at 1, 2, 4 and 5. It is loaded with a vertical point load P at 3.

Use the stiffness method to find the displacements of the structure and hence calculate the support reactions and the forces in all the members. Plot the bending moment diagram for 123. All members have the same section properties and $GJ = 0.8EI$.

Ans. $F_{y,1} = F_{y,5} = -P/16$
$F_{y,2} = F_{y,4} = 9P/16$
$M_{21} = M_{45} = -Pl/16$ (hogging)
$M_{23} = M_{43} = -Pl/12$ (hogging)

Twisting moment in 62, 82, 74 and 94 is $Pl/96$.

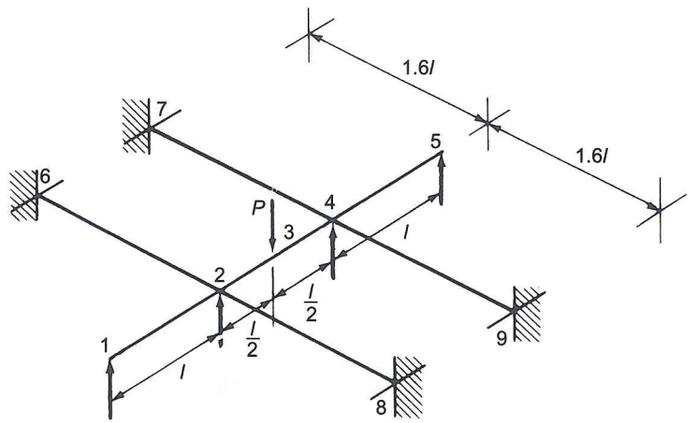

FIGURE P.17.8

17.9 It is required to formulate the stiffness of a triangular element 123 with coordinates (0, 0) (a, 0) and (0, a) respectively, to be used for 'plane stress' problems.

a. Form the [B] matrix.
b. Obtain the stiffness matrix [K^e].

P.17.10 It is required to form the stiffness matrix of a triangular element 123 for use in stress analysis problems. The coordinates of the element are (1, 1), (2, 1) and (2, 2) respectively.

a. Assume a suitable displacement field explaining the reasons for your choice.
b. Form the [B] matrix.
c. Form the matrix which gives, when multiplied by the element nodal displacements, the stresses in the element. Assume a general [D] matrix.

P.17.11 It is required to form the stiffness matrix for a rectangular element of side $2a \times 2b$ and thickness t for use in 'plane stress' problems.

a. Assume a suitable displacement field.
b. Form the [C] matrix.
c. Obtain $\int_{vol}[C]^T[D][C]\,dV$.
Note that the stiffness matrix may be expressed as

$$[K^e] = [A^{-1}]^T \left[\int_{vol} [C]^T[D][C]\,dV \right] [A^{-1}]$$

P.17.12 A square element 1234, whose corners have coordinates x, y (in m) of (−1, −1), (1, −1), (1, 1) and (− 1, 1), respectively, was used in a plane stress finite element analysis. The following nodal displacements (mm) were obtained:

$w_1 = 0.1$	$w_2 = 0.3$	$w_3 = 0.6$	$w_4 = 0.1$
$v_1 = 0.1$	$v_2 = 0.3$	$v_3 = 0.7$	$v_4 = 0.5$

If Young's modulus $E = 200\,000$ N/mm^2 and Poisson's ratio $\nu = 0.3$, calculate the stresses at the centre of the element.

Ans. $\sigma_x = 51.65$ N/mm^2, $\sigma_y = 55.49$ N/mm^2, $\tau_{xy} = 13.46$ N/mm^2.

P.17.13 A triangular element with corners 1, 2 and 3, whose x, y coordinates in metres are (2.0, 3.0), (3.0, 3.0) and (2.5, 4.0), respectively, was used in a plane stress finite element analysis. The following nodal displacements (mm) were obtained.

$$w_1 = 0.04 \quad v_1 = 0.08 \quad w_2 = 0.10 \quad v_2 = 0.12 \quad w_3 = 0.20 \quad v_3 = 0.18$$

Calculate the stresses in the element if Young's modulus is 200 000 N/mm^2 and Poisson's ratio is 0.3.

Ans. $\sigma_x = 25.4$ N/mm^2 $\sigma_y = 28.5$ N/mm^2 $\tau_{xy} = 13.1$ N/mm^2.

P.17.14 A rectangular element 1234 has corners whose x, y coordinates in metres are, respectively, (−2, −1), (2, −1), (2, 1) and (−2, 1). The element was used in a plane stress finite element analysis and the following displacements (mm) were obtained.

	1	2	3	4
w	0.001	0.003	−0.003	0.0
v	−0.004	−0.002	0.001	0.001

If the stiffness of the element was derived assuming a linear variation of displacements, Young's modulus is 200 000 N/mm^2 and Poisson's ratio is 0.3, calculate the stresses at the centre of the element.

Ans. $\sigma_x = 104.4$ N/mm^2 $\sigma_y = 431.3$ N/mm^2 $\tau_{xy} = -115.4$ N/mm^2.

17.15 Derive the stiffness matrix of a constant strain, triangular finite element 123 of thickness t and coordinates (0, 0), (2, 0) and (0, 3), respectively, to be used for plane stress problems. The elements of the elasticity matrix **[D]** are as follows.

$$D_{11} = D_{22} = a \quad D_{12} = b \quad D_{13} = D_{23} = 0 \quad D_{33} = c$$

where a, b and c are material constants.

Ans. See Solutions Manual.

17.16 A constant strain triangular element has corners 1(0,0), 2(4,0) and 3(2,2) and is 1 unit thick. If the elasticity matrix [D] has elements $D_{11} = D_{22} = a$, $D_{12} = D_{21} = b$, $D_{13} = D_{23} = D_{31} = D_{32} = 0$ and $D_{33} = c$, derive the stiffness matrix for the element.

Ans.

$$[K^e] = \frac{1}{4}\begin{bmatrix} a+c & & & & & \\ b+c & a+c & & & & \\ -a+c & -b+c & a+c & & & \\ b-c & a-c & -b-c & a+c & & \\ -2c & -2c & -2c & 2c & 4c & \\ -2b & -2a & 2b & -2a & 0 & 4a \end{bmatrix}$$

17.17 The following interpolation formula is suggested as a displacement function for deriving the stiffness matrix of a plane stress rectangular element of uniform thickness t shown in Fig P.17.17

$$u = \frac{1}{4ab}\left[(a-x)(b-y)u_1 + (a+x)(b-y)u_2 + (a+x)(b+y)u_3 + (a-x)(b+y)u_4\right]$$

Form the strain matrix and obtain the stiffness coefficients K_{11} and K_{12} in terms of the material constants c, d and e where, in the elasticity matrix [D], $D_{11} = D_{22} = c$, $D_{12} = d$, $D_{33} = e$ and $D_{13} = D_{23} = 0$.

Ans. $K_{11} = t(4c + e)/6$, $K_{12} = t(d + e)/4$

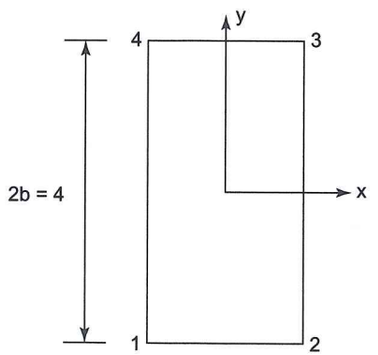

CHAPTER

Plastic Analysis of Beams and Frames

18

So far our analysis of the behaviour of structures has assumed that whether the structures are statically determinate or indeterminate the loads on them cause stresses which lie within the elastic limit. Design, based on this elastic behaviour, ensures that the greatest stress in a structure does not exceed the yield stress divided by an appropriate factor of safety.

An alternative approach is based on *plastic analysis* in which the loads required to cause the structure to *collapse* are calculated. The reasoning behind this method is that, in most steel structures, particularly redundant ones, the loads required to cause the structure to collapse are somewhat larger than the ones which cause yielding. Design, based on this method, calculates the loading required to cause complete collapse and then ensures that this load is greater than the applied loading; the ratio of collapse load to the maximum applied load is called the *load factor*. Generally, *plastic,* or *ultimate load* design, results in more economical structures.

In this chapter we shall investigate the mechanisms of plastic collapse and determine collapse loads for a variety of beams and frames.

18.1 Theorems of plastic analysis

Plastic analysis is governed by three fundamental theorems which are valid for elasto-plastic structures in which the displacements are small such that the geometry of the displaced structure does not affect the applied loading system.

The uniqueness theorem

The following conditions must be satisfied simultaneously by a structure in its collapsed state:

The *equilibrium condition* states that the bending moments must be in equilibrium with the applied loads.

The *yield condition* states that the bending moment at any point in the structure must not exceed the plastic moment at that point.

The *mechanism condition* states that sufficient plastic hinges must have formed so that all, or part of, the structure is a mechanism.

The lower bound, or safe, theorem

If a distribution of moments can be found which satisfies the above equilibrium and yield conditions the structure is either safe or just on the point of collapse.

upper bound, or unsafe, theorem

loading is found which causes a collapse mechanism to form then the loading must be equal to or ter than the actual collapse load.

Generally, in plastic analysis, the upper bound theorem is used. Possible collapse mechanisms are ılated and the corresponding collapse loads calculated. From the upper bound theorem we know all mechanisms must give a value of collapse load which is greater than or equal to the true collapse so that the critical mechanism is the one giving the lowest load. It is possible that a mechanism, ch would give a lower value of collapse load, has been missed. A check must therefore be carried by applying the lower bound theorem.

.2 Plastic analysis of beams

erally plastic behaviour is complex and is governed by the form of the stress–strain curve in tension compression of the material of the beam. Fortunately mild steel beams, which are used extensively ivil engineering construction, possess structural properties that lend themselves to a relatively simple ysis of plastic bending.

We have seen in Section 8.3, Fig. 8.8, that mild steel obeys Hooke's law up to a sharply defined l stress and then undergoes large strains during yielding until strain hardening causes an increase in s. For the purpose of plastic analysis we shall neglect the upper and lower yield points and idealize stress–strain curve as shown in Fig. 18.1. We shall also neglect the effects of strain hardening, but e this provides an increase in strength of the steel it is on the safe side to do so. Finally we shall me that both Young's modulus, E, and the yield stress, σ_Y, have the same values in tension and pression, and that plane sections remain plane after bending. The last assumption may be shown erimentally to be very nearly true.

stic bending of beams having a singly symmetrical cross section

s is the most general case we shall discuss since the plastic bending of beams of arbitrary section is plex and is still being researched.

Consider the length of beam shown in Fig. 18.2(a) subjected to a positive bending moment, M, possessing the singly symmetrical cross section shown in Fig. 18.2(b). If M is sufficiently small the th of beam will bend elastically, producing at any section mm, the linear direct stress distribution ig. 18.2(c) where the stress, σ, at a distance y from the neutral axis of the beam is given by

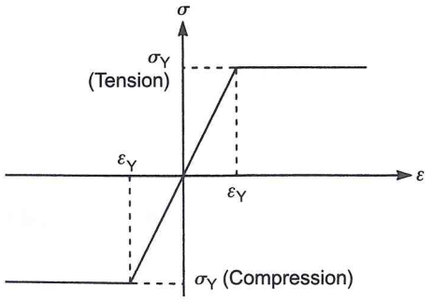

FIGURE 18.1

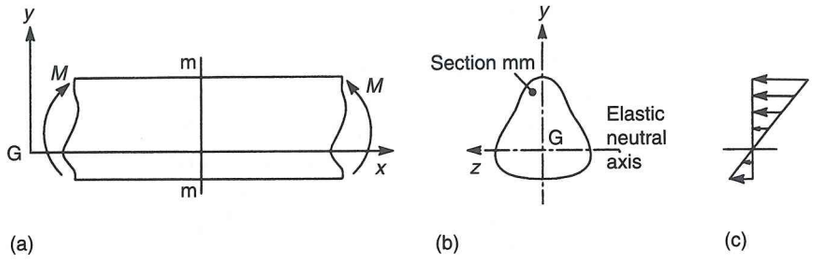

FIGURE 18.2

Direct stress due to bending in a singly symmetrical section beam.

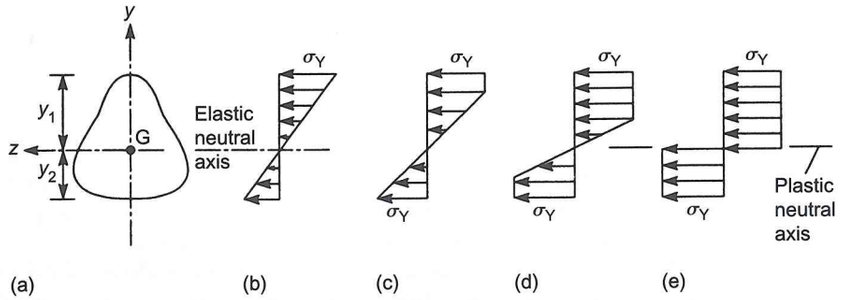

FIGURE 18.3

Yielding of a beam section due to bending.

Eq. (9.9). In this situation the *elastic neutral axis* of the beam section passes through the centroid of area of the section (Eq. (9.5)).

Suppose now that M is increased. A stage will be reached where the maximum direct stress in the section, i.e. at the point furthest from the elastic neutral axis, is equal to the yield stress, σ_Y (Fig. 18.3 (b)). The corresponding value of M is called the *yield moment*, M_Y, and is given by Eq. (9.9); thus

$$M_Y = \frac{\sigma_Y I}{y_1} \tag{18.1}$$

If the bending moment is further increased, the strain at the extremity y_1 of the section increases and exceeds the yield strain, ε_Y. However, due to plastic yielding the stress remains constant and equal to σ_Y as shown in the idealized stress–strain curve of Fig. 18.1. At some further value of M the stress at the lower extremity of the section also reaches the yield stress, σ_Y (Fig. 18.3(c)). Subsequent increases in bending moment cause the regions of plasticity at the extremities of the beam section to extend inwards, producing a situation similar to that shown in Fig. 18.3(d); at this stage the central portion or 'core' of the beam section remains elastic while the outer portions are plastic. Finally, with further increases in bending moment the elastic core is reduced to a negligible size and the beam section is more or less completely plastic. Then, for all practical purposes the beam has reached its ultimate moment resisting capacity; the value of bending moment at this stage is known as the *plastic moment*, M_P, of the beam. The stress distribution corresponding to this moment may be idealized into two rect-

The problem now, therefore, is to determine the plastic moment, M_P. First, however, we must vestigate the position of the neutral axis of the beam section when the latter is in its fully plastic state. ne of the conditions used in establishing that the elastic neutral axis coincides with the centroid of a :am section was that stress is directly proportional to strain (Eq. (9.2)). It is clear that this is no longer e case for the stress distributions of Figs 18.3(c), (d) and (e). In Fig. 18.3(e) the beam section above e *plastic neutral axis* is subjected to a uniform compressive stress, σ_Y, while below the neutral axis the :ess is tensile and also equal to σ_Y. Suppose that the area of the beam section below the plastic neutral is is A_2, and that above, A_1 (Fig. 18.4(a)). Since M_P is a pure bending moment the total direct load ı the beam section must be zero. Thus from Fig. 18.4

$$\sigma_Y A_1 = \sigma_Y A_2$$

that

$$A_1 = A_2 \tag{18.2}$$

ıerefore if the total cross-sectional area of the beam section is A

$$A_1 = A_2 = \frac{A}{2} \tag{18.3}$$

d we see that the plastic neutral axis divides the beam section into two equal areas. Clearly for doubly ınmetrical sections or for singly symmetrical sections in which the plane of the bending moment is rpendicular to the axis of symmetry, the elastic and plastic neutral axes coincide.

The plastic moment, M_P, can now be found by taking moments of the resultants of the tensile and mpressive stresses about the neutral axis. These stress resultants act at the centroids C_1 and C_2 of the :as A_1 and A_2, respectively. Thus from Fig. 18.4

$$M_P = \sigma_Y A_1 \bar{y}_1 + \sigma_Y A_2 \bar{y}_2$$

using Eq. (18.3)

$$M_P = \sigma_Y \frac{A}{2} (\bar{y}_1 + \bar{y}_2) \tag{18.4}$$

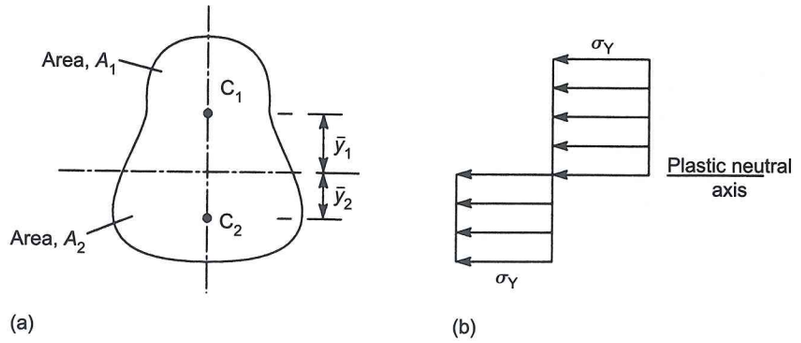

URE 18.4

ition of the plastic neutral axis in a beam section

Equation (18.4) may be written in a similar form to Eq. (9.13); thus

$$M_P = \sigma_Y Z_P \tag{18.5}$$

where

$$Z_P = \frac{A(\bar{y}_1 + \bar{y}_2)}{2} \tag{18.6}$$

Z_P is known as the *plastic modulus* of the cross section. Note that the elastic modulus, Z_e, has two values for a beam of singly symmetrical cross section (Eq. (9.12)) whereas the plastic modulus is single-valued.

Shape factor

The ratio of the plastic moment of a beam to its yield moment is known as the *shape factor, f.* Thus

$$f = \frac{M_P}{M_Y} = \frac{\sigma_Y Z_P}{\sigma_Y Z_e} = \frac{Z_P}{Z_e} \tag{18.7}$$

where Z_P is given by Eq. (18.6) and Z_e is the minimum elastic section modulus, I/y_1. It can be seen from Eq. (18.7) that f is solely a function of the geometry of the beam cross section.

EXAMPLE 18.1

Determine the yield moment, the plastic moment and the shape factor for a rectangular section beam of breadth b and depth d.

The elastic and plastic neutral axes of a rectangular cross section coincide (Eq. (18.3)) and pass through the centroid of area of the section. Thus, from Eq. (18.1)

$$M_Y = \frac{\sigma_Y bd^3/12}{d/2} = \sigma_Y \frac{bd^2}{6} \tag{i}$$

and from Eq. (18.4)

$$M_P = \sigma_Y \frac{bd}{2}\left(\frac{d}{4} + \frac{d}{4}\right) = \sigma_Y \frac{bd^2}{4} \tag{ii}$$

Substituting for M_P and M_Y in Eq. (18.7) we obtain

$$f = \frac{M_P}{M_Y} = \frac{3}{2} \tag{iii}$$

Note that the plastic collapse of a rectangular section beam occurs at a bending moment that is 50% greater than the moment at initial yielding of the beam.

EXAMPLE 18.2

Determine the shape factor for the I-section beam shown in Fig. 18.5(a).

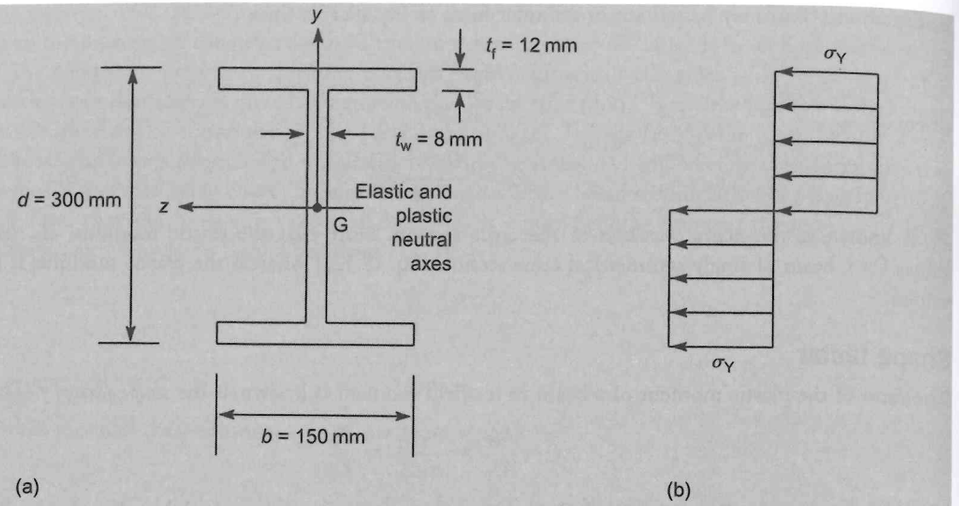

URE 18.5

am section of Ex. 18.2.

Again, as in Ex. 18.1, the elastic and plastic neutral axes coincide with the centroid, G, of the tion.

In the fully plastic condition the stress distribution in the beam is that shown in Fig. 18.5(b). e total direct force in the upper flange is

$$\sigma_Y b t_f \text{ (compression)}$$

l its moment about Gz is

$$\sigma_Y b t_f \left(\frac{d}{2} - \frac{t_f}{2}\right) \equiv \frac{\sigma_Y b t_f}{2}(d - t_f) \tag{i}$$

Similarly the total direct force in the web above Gz is

$$\sigma_Y t_w \left(\frac{d}{2} - t_f\right) \text{ (compression)}$$

l its moment about Gz is

$$\sigma_Y t_w \left(\frac{d}{2} - t_f\right)\frac{1}{2}\left(\frac{d}{2} - t_f\right) \equiv \frac{\sigma_Y t_w}{8}(d - 2t_f)^2 \tag{ii}$$

The lower half of the section is in tension and contributes the same moment about Gz so that total plastic moment, M_P, of the complete section is given by

$$M_P = \sigma_Y \left[b t_f (d - t_f) + \frac{1}{4} t_w (d - 2t_f)^2\right] \tag{iii}$$

Comparing Eqs. (18.5) and (iii) we see that Z_P is given by

$$Z_P = b t_f (d - t_f) + \frac{1}{4} t_w (d - 2t_f)^2 \tag{iv}$$

Alternatively we could have obtained Z_P from Eq. (18.6).

The second moment of area, I, of the section about the common neutral axis is

$$I = \frac{bd^3}{12} - \frac{(b - t_w)(d - 2t_f)^3}{12}$$

so that the elastic modulus Z_e is given by

$$Z_e = \frac{I}{d/2} = \frac{2}{d}\left[\frac{bd^3}{12} - \frac{(b - t_w)(d - 2t_f)^3}{12}\right] \tag{v}$$

Substituting the actual values of the dimensions of the section in Eqs (iv) and (v) we obtain

$$Z_P = 150 \times 12(300 - 12) + \frac{1}{4} \times 8(300 - 2 \times 12)^2 = 6.7 \times 10^5 \text{mm}^3$$

and

$$Z_e = \frac{2}{300}\left[\frac{150 \times 300^3}{12} - \frac{(150 - 8)(300 - 24)^3}{12}\right] = 5.9 \times 10^5 \text{mm}^3$$

Therefore from Eq. (18.7)

$$f = \frac{M_P}{M_Y} = \frac{Z_P}{Z_e} = \frac{6.7 \times 10^5}{5.9 \times 10^5} = 1.14$$

and we see that the fully plastic moment is only 14% greater than the moment at initial yielding.

EXAMPLE 18.3

Determine the shape factor of the T-section shown in Fig. 18.6.

In this case the elastic and plastic neutral axes are not coincident. Suppose that the former is a depth y_e from the upper surface of the flange and the latter a depth y_P. The elastic neutral axis passes through the centroid of the section, the location of which is found in the usual way. Hence, taking moments of areas about the upper surface of the flange

$$(150 \times 10 + 190 \times 7)y_e = 150 \times 10 \times 5 + 190 \times 7 \times 105$$

which gives

$$y_e = 52.0 \text{ mm}$$

The second moment of area of the section about the elastic neutral axis is then, using Eq. (9.38)

$$I = \frac{150 \times 52^3}{3} - \frac{143 \times 42^3}{3} + \frac{7 \times 148^3}{3} = 11.1 \times 10^6 \text{ mm}^4$$

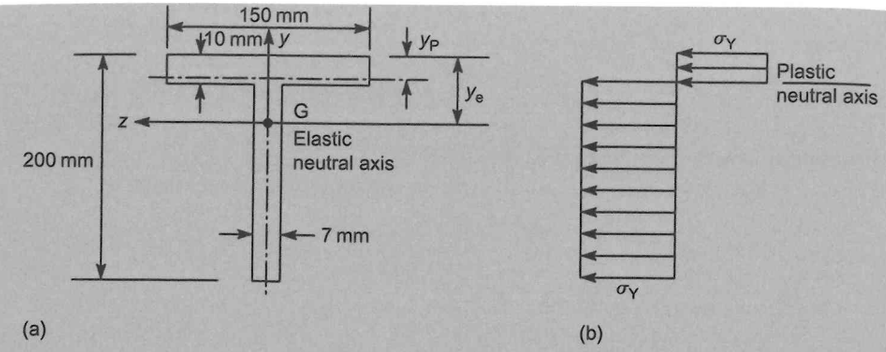

FIGURE 18.6
Beam section of Ex. 18.3.

Therefore

$$Z_e = \frac{11.1 \times 10^6}{148} = 75\,000 \text{ mm}^3$$

Note that we choose the least value for Z_e since the stress will be a maximum at a point furthest from the elastic neutral axis.

The plastic neutral axis divides the section into equal areas (see Eq. (18.3)). Inspection of Fig. 18.6 shows that the flange area is greater than the web area so that the plastic neutral axis must lie within the flange. Hence

$$150y_P = 150(10 - y_P) + 190 \times 7$$

from which

$$y_P = 9.4 \text{ mm}$$

Equation (18.6) may be interpreted as the first moment, about the plastic neutral axis, of the area above the plastic neutral axis plus the first moment of the area below the plastic neutral axis. Hence

$$Z_P = 150 \times 9.4 \times 4.7 + 150 \times 0.6 \times 0.3 + 190 \times 7 \times 95.6 = 133\,800 \text{ mm}^3$$

The shape factor f is, from Eq. (18.7)

$$f = \frac{M_P}{M_Y} = \frac{Z_P}{Z_e} = \frac{133\,800}{75\,000} = 1.78$$

oment–curvature relationships

om Eq. (9.8) we see that the curvature k of a beam subjected to elastic bending is given by

$$k = \frac{1}{R} = \frac{M}{EI} \tag{18.8}$$

At yield, when M is equal to the yield moment, M_Y

$$k_Y = \frac{M_Y}{EI} \tag{18.9}$$

The moment–curvature relationship for a beam in the linear elastic range may therefore be expressed in non-dimensional form by combining Eqs (18.8) and (18.9), i.e.

$$\frac{M}{M_Y} = \frac{k}{k_Y} \tag{18.10}$$

This relationship is represented by the linear portion of the moment–curvature diagram shown in Fig. 18.7. When the bending moment is greater than M_Y part of the beam becomes fully plastic and the moment–curvature relationship is non-linear. As the plastic region in the beam section extends inwards towards the neutral axis the curve becomes flatter as rapid increases in curvature are produced by small increases in moment. Finally, the moment–curvature curve approaches the horizontal line $M = M_P$ as an asymptote when, theoretically, the curvature is infinite at the collapse load. From Eq. (18.7) we see that when $M = M_P$, the ratio $M/M_Y = f$, the shape factor. Clearly the equation of the non-linear portion of the moment–curvature diagram depends upon the particular cross section being considered.

Suppose a beam of rectangular cross section is subjected to a bending moment which produces fully plastic zones in the outer portions of the section (Fig. 18.8(a)); the depth of the elastic core is d_e. The total bending moment, M, corresponding to the stress distribution of Fig. 18.8(b) is given by

$$M = 2\sigma_Y b \frac{1}{2}(d - d_e)\frac{1}{2}\left(\frac{d}{2} + \frac{d_e}{2}\right) + 2\frac{\sigma_Y}{2} b \frac{d_e}{2}\frac{2}{3}\frac{d_e}{2}$$

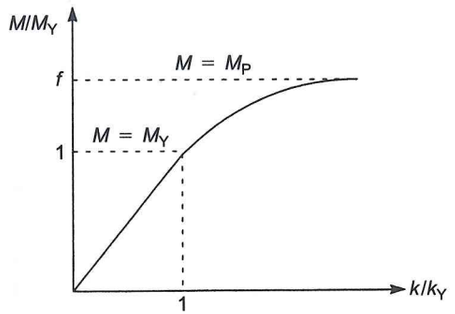

FIGURE 18.7
Moment–curvature diagram for a beam.

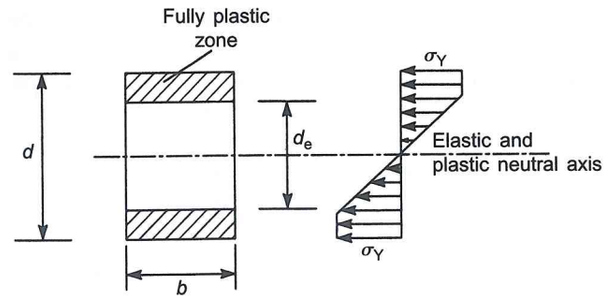

FIGURE 18.8
Plastic bending of a rectangular-section

ich simplifies to

$$M = \frac{\sigma_Y b d^2}{12}\left(3 - \frac{d_e^2}{d^2}\right) = \frac{M_Y}{2}\left(3 - \frac{d_e^2}{d^2}\right) \tag{18.11}$$

te that when $d_e = d$, $M = M_Y$ and when $d_e = 0$, $M = 3M_Y/2 = M_P$ as derived in Ex. 18.1.

The curvature of the beam at the section shown may be found using Eq. (9.2) and applying it to a nt on the outer edge of the elastic core. Thus

$$\sigma_Y = E\frac{d_e}{2R}$$

$$k = \frac{1}{R} = \frac{2\sigma_Y}{Ed_e} \tag{18.12}$$

e curvature of the beam at yield is obtained from Eq. (18.9), i.e.

$$k_Y = \frac{M_Y}{EI} = \frac{2\sigma_Y}{Ed} \tag{18.13}$$

mbining Eqs (18.12) and (18.13) we obtain

$$\frac{k}{k_Y} = \frac{d}{d_e} \tag{18.14}$$

stituting for d_e/d in Eq. (18.11) from Eq. (18.14) we have

$$M = \frac{M_Y}{2}\left(3 - \frac{k_Y^2}{k^2}\right)$$

hat

$$\frac{k}{k_Y} = \frac{1}{\sqrt{3 - 2M/M_Y}} \tag{18.15}$$

ation (18.15) gives the moment–curvature relationship for a rectangular section beam for $\leq M \leq M_P$, i.e. for the non-linear portion of the moment–curvature diagram of Fig. 18.7 for the icular case of a rectangular section beam. Corresponding relationships for beams of different section found in a similar manner.

We have seen that for bending moments in the range $M_Y \leq M \leq M_P$ a beam section comprises fully tic regions and a central elastic core. Thus yielding occurs in the plastic regions with no increase in stress reas in the elastic core increases in deformation are accompanied by increases in stress. The deformation he beam is therefore controlled by the elastic core, a state sometimes termed *contained plastic flow. As M* roaches M_P the moment–curvature diagram is asymptotic to the line $M = M_P$ so that large increases in rmation occur without any increase in moment, a condition known as *unrestricted plastic flow.*

In Eq. (iii) of Ex. 18.1 we have seen that, for a rectangular section beam, the ratio of the plastic ment to the yield moment is 1.5:1, that is

$$M_Y = \frac{2}{3}M_P$$

Then, substituting for M_Y in Eq. (18.15) and rearranging we obtain

$$M = \left[1 - \frac{1}{3}\left(\frac{k_Y}{k}\right)^2\right]M_P$$

For a range of values of k_Y/k we can obtain the applied moment in terms of the plastic moment as shown in Table 18.1.

Therefore we see that when the applied moment is approaching 99% of the plastic moment the beam curvature is only five times greater than that at the onset of yield.

Plastic hinges

The presence of unrestricted plastic flow at a section of a beam leads us to the concept of the formation of *plastic hinges* in beams and other structures.

Consider the simply supported beam shown in Fig. 18.9(a); the beam carries a concentrated load, W, at mid-span. The bending moment diagram (Fig. 18.9(b)) is triangular in shape with a maximum moment equal to $WL/4$. If W is increased in value until $WL/4 = M_P$, the mid-span section of the beam will be fully plastic with regions of plasticity extending towards the supports as the bending moment decreases; no plasticity occurs in beam sections for which the bending moment is less than M_Y. Clearly, unrestricted plastic flow now occurs at the mid-span section where large increases in deformation take place with no increase in load. The beam therefore behaves as two rigid beams connected by a *plastic*

Table 18.1

k/k_Y	1	2	3	4	5
M/M_P	0.667	0.917	0.963	0.979	0.987

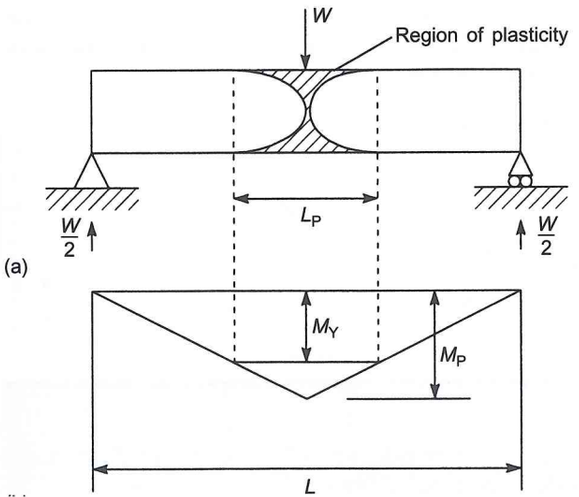

FIGURE 18.9
Formation of a plastic hinge in a simply

ge which allows them to rotate relative to each other. The value of W given by $W = 4M_P/L$ is the *col-se load* for the beam.

The length, L_P, of the plastic region of the beam may be found using the fact that at each section inding the region the bending moment is equal to M_Y. Thus

$$M_Y = \frac{W}{2}\left(\frac{L - L_P}{2}\right)$$

ostituting for $W(=4M_P/L)$ we obtain

$$M_Y = \frac{M_P}{L}(L - L_P)$$

n which

$$L_P = L\left(1 - \frac{M_Y}{M_P}\right)$$

from Eq. (18.7)

$$L_P = L\left(1 - \frac{1}{f}\right) \tag{18.16}$$

a rectangular section beam $f = 1.5$ (see Ex. 18.1), giving $L_P = L/3$. For the I-section beam of Ex. 2, $f = 1.14$ and $L_P = 0.12L$ so that the plastic region in this case is much smaller than that of a rect-ular section beam; this is generally true for I-section beams.

It is clear from the above that plastic hinges form at sections of maximum bending moment.

istic analysis of beams

can now use the concept of plastic hinges to determine the collapse or ultimate load of beams in ns of their individual yield moment, M_P, which may be found for a particular beam section using (18.5).

For the case of the simply supported beam of Fig. 18.9 we have seen that the formation of a single plastic ge is sufficient to produce failure; this is true for all statically determinate systems. Having located the posi-n of the plastic hinge, at which the moment is equal to M_P, the collapse load is found from simple statics. as for the beam of Fig. 18.9, taking moments about the mid-span section, we have

$$\frac{W_U}{2}\frac{L}{2} = M_P$$

$$W_U = \frac{4M_P}{L} \text{ (as deduced before)}$$

ere W_U is the ultimate value of the load W.

XAMPLE 18.4

etermine the ultimate load for a simply supported, rectangular section beam, breadth b, depth d, ving a span L and subjected to a uniformly distributed load of intensity w.

The maximum bending moment occurs at mid-span and is equal to $wL^2/8$ (see Section 3.4). The plastic hinge therefore forms at mid-span when this bending moment is equal to M_P, the corresponding ultimate load intensity being w_U. Thus

$$\frac{w_U L^2}{8} = M_P \tag{i}$$

From Ex. 18.1, Eq. (ii)

$$M_P = \sigma_Y \frac{bd^2}{4}$$

so that

$$w_U = \frac{8M_P}{L^2} = \frac{2\sigma_Y bd^2}{L^2}$$

where σ_Y is the yield stress of the material of the beam.

EXAMPLE 18.5

The simply supported beam ABC shown in Fig. 18.10(a) has a cantilever overhang and supports loads of $4W$ and W. Determine the value of W at collapse in terms of the plastic moment, M_P, of the beam.

The bending moment diagram for the beam is constructed using the method of Section 3.4 and is shown in Fig. 18.10(b). Clearly as W is increased a plastic hinge will form first at D, the point of application of the $4W$ load. Thus, at collapse

$$\frac{3}{4}W_U L = M_P$$

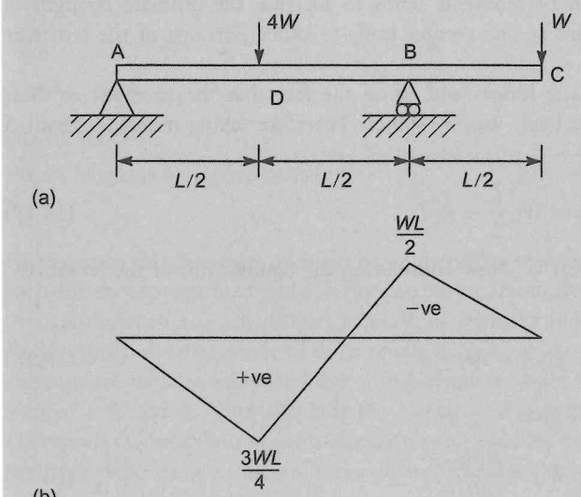

FIGURE 18.10
Beam of Ex. 18.5.

so that

$$W_U = \frac{4M_P}{3L}$$

where W_U is the value of W that causes collapse.

The formation of a plastic hinge in a statically determinate beam produces large, increasing deformaons which ultimately result in failure with no increase in load. In this condition the beam behaves as mechanism with different lengths of beam rotating relative to each other about the plastic hinge. The rms *failure mechanism* or *collapse mechanism* are often used to describe this state.

In a statically indeterminate system the formation of a single plastic hinge does not necessarily mean llapse. Consider the propped cantilever shown in Fig. 18.11(a). The bending moment diagram may drawn after the reaction at C has been determined by any suitable method of analysis of statically determinate beams (see Chapter 16) and is shown in Fig. 18.11(b).

As the value of W is increased a plastic hinge will form first at A where the bending moment is eatest. However, this does not mean that the beam will collapse. Instead it behaves as a statically terminate beam with a point load at B and a moment M_P at A. Further increases in W eventually ult in the formation of a second plastic hinge at B (Fig. 18.11(c)) when the bending moment at B ches the value M_P. The beam now behaves as a mechanism and failure occurs with no further rease in load. The bending moment diagram for the beam is now as shown in Fig. 18.11(d) with ues of bending moment of $-M_P$ at A and M_P at B. Comparing the bending moment diagram at lapse with that corresponding to the elastic deformation of the beam (Fig. 18.11(b)) we see that a listribution of bending moment has occurred. This is generally the case in statically indeterminate tems whereas in statically determinate systems the bending moment diagrams in the elastic range l at collapse have identical shapes (see Figs. 18.9(b) and 18.10(b)). In the beam of Fig. 18.11 the stic bending moment diagram has a maximum at A. After the formation of the plastic hinge at A bending moment remains constant while the bending moment at B increases until the second stic hinge forms. Thus this redistribution of moments tends to increase the ultimate strength of ically indeterminate structures since failure at one section leads to other portions of the structure porting additional load.

Having located the positions of the plastic hinges and using the fact that the moment at these ges is M_P, we may determine the ultimate load, W_U, by statics. Therefore taking moments about A have

$$M_P = W_U \frac{L}{2} - R_C L \tag{18.17}$$

re R_C is the vertical reaction at the support C. Now considering the equilibrium of the length BC btain

$$R_C \frac{L}{2} = M_P \tag{18.18}$$

inating R_C from Eqs (18.17) and (18.18) gives

$$W_U = \frac{6M_P}{L} \tag{18.19}$$

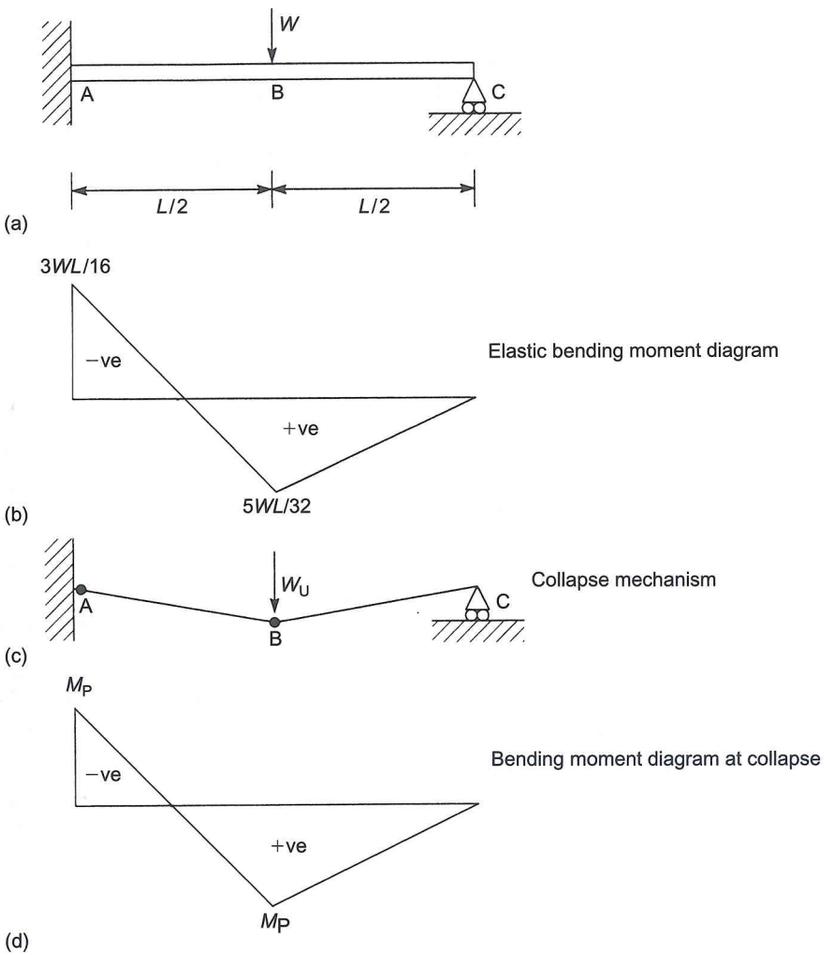

FIGURE 18.11
Plastic hinges in a propped cantilever.

Note that in this particular problem it is unnecessary to determine the elastic bending moment diagram to solve for the ultimate load which is obtained using statics alone. This is a convenient feature of plastic analysis and leads to a much simpler solution of statically indeterminate structures than an elastic analysis. Furthermore, the magnitude of the ultimate load is not affected by structural imperfections such as a sinking support, whereas the same kind of imperfection would have an appreciable effect on the elastic behaviour of a structure. Note also that the principle of superposition (Section 3.7), which is based on the linearly elastic behaviour of a structure, does not hold for plastic analysis. In fact the plastic behaviour of a structure depends upon the order in which the loads are applied as well as their final values. We therefore assume in plastic analysis that all loads are applied simultaneously and that the ratio of the loads remains

An alternative and powerful method of analysis uses the principle of virtual work (see Section 15.2), ch states that for a structure that is in equilibrium and which is given a small virtual displacement, sum of the work done by the internal forces is equal to the work done by the external forces.

Consider the propped cantilever of Fig. 18.11(a); its collapse mechanism is shown in Fig. 18.11(c). the instant of collapse the cantilever is in equilibrium with plastic hinges at A and B where the ments are each M_P as shown in Fig. 18.11(d). Suppose that AB is given a small rotation, θ. From metry, BC also rotates through an angle θ as shown in Fig. 18.12; the vertical displacement of B is ı $\theta L/2$. The external forces on the cantilever which do work during the virtual displacement are com- ed solely of W_U since the vertical reactions at A and C are not displaced. The internal forces which do k consist of the plastic moments, M_P, at A and B and which resist rotation. Hence

$$W_U\theta\frac{L}{2} = (M_P)_A\theta + (M_P)_B 2\theta \text{ (see Section 15.1)}$$

n which $W_U = 6M_P/L$ as before.

We have seen that the plastic hinges form at beam sections where the bending moment diagram ins a peak value. It follows that for beams carrying a series of point loads, plastic hinges are located he load positions. However, in some instances several collapse mechanisms are possible, each giving erent values of ultimate load. For example, if the propped cantilever of Fig. 18.11(a) supports two ıt loads as shown in Fig. 18.13(a), three possible collapse mechanisms are possible (Fig. 18.13 d). Each possible collapse mechanism should be analysed and the lowest ultimate load selected.

The beams we have considered so far have carried concentrated loads only so that the positions of plastic hinges, and therefore the form of the collapse mechanisms, are easily determined. This is not case when distributed loads are involved.

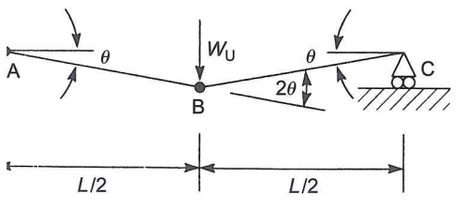

RE 18.12

ıal displacements in propped cantilever of

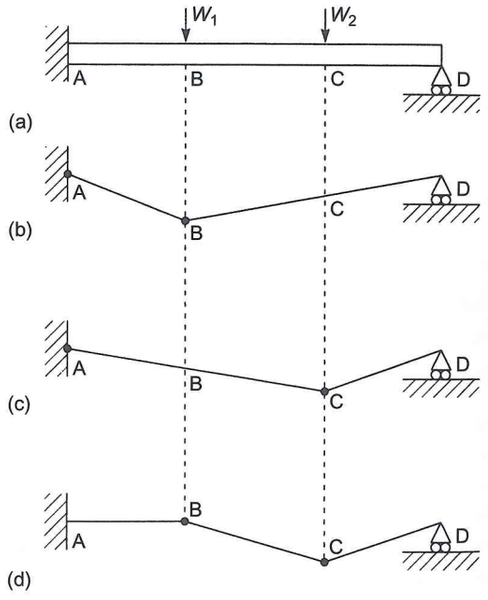

FIGURE 18.13

Possible collapse mechanisms in a propped cantilever

EXAMPLE 18.6

The propped cantilever AB shown in Fig. 18.14(a) carries a uniformly distributed load of intensity w. If the plastic moment of the cantilever is M_P calculate the minimum value of w required to cause collapse.

Peak values of bending moment occur at A and at some point between A and B so that plastic hinges will form at A and at a point C a distance x, say, from A; the collapse mechanism is then as shown in Fig. 18.14(b) where the rotations of AC and CB are θ and ϕ respectively. Then, the vertical deflection of C is given by

$$\delta = \theta x = \phi(L - x) \tag{i}$$

so that

$$\phi = \theta\frac{x}{L-x} \tag{ii}$$

The total load on AC is wx and its centroid (at $x/2$ from A) will be displaced a vertical distance $\delta/2$. The total load on CB is $w(L - x)$ and its centroid will suffer the same vertical displacement $\delta/2$. Then, from the principle of virtual work

$$wx\frac{\delta}{2} + w(L-x)\frac{\delta}{2} = M_P\theta + M_P(\theta + \phi)$$

Note that the beam at B is free to rotate so that there is no plastic hinge at B. Substituting for δ from Eq. (i) and ϕ from Eq. (ii) we obtain

$$wL\frac{\theta x}{2} = M_P\theta + M_P\left(\theta + \theta\frac{x}{L-x}\right)$$

or

$$wL\frac{\theta x}{2} = M_P\theta\left(2 + \frac{x}{L-x}\right)$$

Rearranging

$$w = \frac{2M_P}{Lx}\left(\frac{2L-x}{L-x}\right) \tag{iii}$$

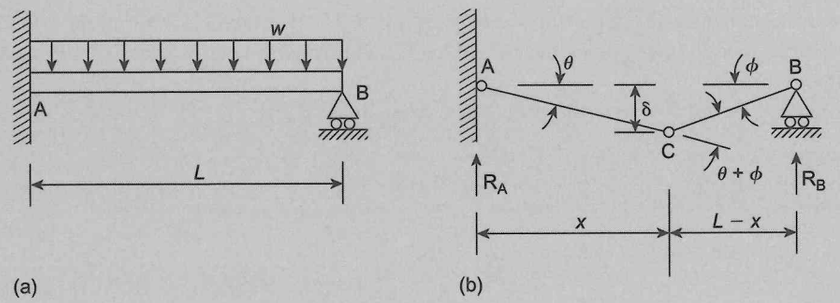

FIGURE 18.14

Collapse mechanism for a propped cantilever.

a minimum value of w, $(dw/dx) = 0$. Then

$$\frac{dw}{dx} = \frac{2M_P}{L}\left[\frac{-x(L-x)-(2L-x)(L-2x)}{x^2(L-x)^2}\right] = 0$$

reduces to

$$x^2 - 4Lx + 2L^2 = 0$$

g gives

$$x = 0.586L \text{ (the positive root is ignored)}$$

en substituting for x in Eq. (iii)

$$w \text{ (at collapse)} = \frac{11.66M_P}{L^2}$$

can now use the lower bound theorem to check that we have obtained the critical mechanism ereby the critical load. The internal moment at A at collapse is hogging and equal to M_P. taking moments about A

$$R_B L - w\frac{L^2}{2} = -M_P$$

gives

$$R_B = \frac{4.83M_P}{L}$$

ilarly, taking moments about B gives

$$R_A = \frac{6.83M_P}{L}$$

mation of R_A and R_B gives $11.66M_P/L = wL$ so that vertical equilibrium is satisfied. Further, ering moments of forces to the right of C about C we have

$$M_C = R_B(0.414L) - w\frac{0.414L^2}{2}$$

stituting for R_B and w from the above gives $M_C = M_P$. The same result is obtained by consid- noments about C of forces to the left of C. The load therefore satisfies both vertical and nt equilibrium.

bending moment at any distance x_1, say, from B is given by

$$M = R_B x_1 - w\frac{x_1^2}{2}$$

$$\frac{dM}{dx_1} = R_B - wx_1 = 0$$

a maximum occurs when $x_1 = R_B/w$. Substituting for R_B, x_1 and w in the expression for M

Plastic design of beams

It is now clear that the essential difference between the plastic and elastic methods of design is that the former produces a structure having a more or less uniform factor of safety against collapse of all its components, whereas the latter produces a uniform factor of safety against yielding. The former method in fact gives an indication of the true factor of safety against collapse of the structure which may occur at loads only marginally greater than the yield load, depending on the cross sections used. For example, a rectangular section mild steel beam has an ultimate strength 50% greater than its yield strength (see Ex. 18.1), whereas for an I-section beam the margin is in the range 10–20% (see Ex. 18.2). It is also clear that each method of design will produce a different section for a given structural component. This distinction may be more readily understood by referring to the redistribution of bending moment produced by the plastic collapse of a statically indeterminate beam.

Two approaches to the plastic design of beams are indicated by the previous analysis. The most direct method would calculate the working loads, determine the required strength of the beam by the application of a suitable load factor, obtain by a suitable analysis the required plastic moment in terms of the ultimate load and finally, knowing the yield stress of the material of the beam, determine the required plastic section modulus. An appropriate beam section is then selected from a handbook of structural sections. The alternative method would assume a beam section, calculate the plastic moment of the section and hence the ultimate load for the beam. This value of ultimate load is then compared with the working loads to determine the actual load factor, which would then be checked against the prescribed value.

EXAMPLE 18.7

The propped cantilever of Fig. 18.11(a) is 10 m long and is required to carry a load of 100 kN at mid-span. If the yield stress of mild steel is 300 N/mm^2, suggest a suitable section using a load factor against failure of 1.5.

The required ultimate load of the beam is $1.5 \times 100 = 150$ kN. Then from Eq. (18.19) the required plastic moment M_P is given by

$$M_P = \frac{150 \times 10}{6} = 250 \text{ kN m}$$

From Eq. (18.5) the minimum plastic modulus of the beam section is

$$Z_P = \frac{250 \times 10^6}{300} = 833\,333 \text{ mm}^3$$

Referring to an appropriate handbook we see that a Universal Beam, 406 mm × 140 mm × 46 kg/m, has a plastic modulus of 886.3 cm^3. This section therefore possesses the required ultimate strength and includes a margin to allow for its self-weight. Note that unless some allowance has been made for self-weight in the estimate of the working loads the design should be rechecked to include this effect.

Effect of axial load on plastic moment

We shall investigate the effect of axial load on plastic moment with particular reference to an I-section beam, one of the most common structural shapes, which is subjected to a positive bending moment

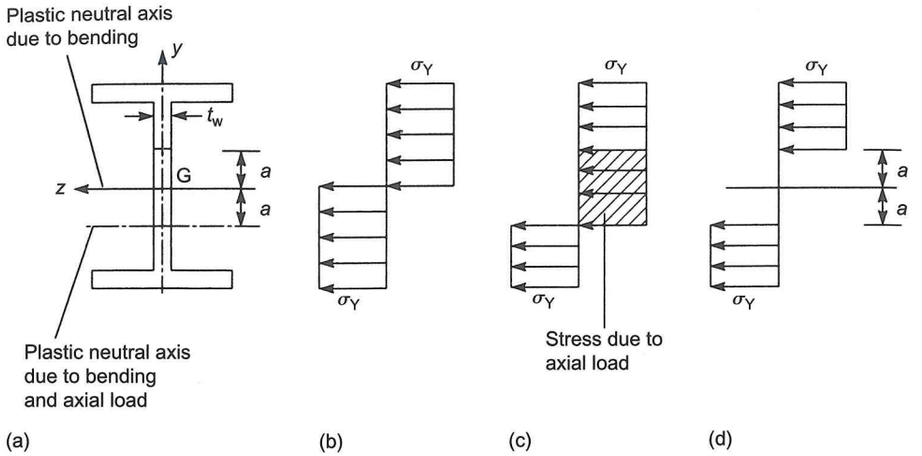

URE 18.15

nbined bending and axial compression.

If the beam section were subjected to its plastic moment only, the stress distribution shown in . 18.15(b) would result. However, the presence of the axial load causes additional stresses which can-, obviously, be greater than σ_Y. Thus the region of the beam section supporting compressive stresses ncreased in area while the region subjected to tensile stresses is decreased in area. Clearly some of the npressive stresses are due to bending and some due to axial load so that the modified stress distribu-1 is as shown in Fig. 18.15(c).

Since the beam section is doubly symmetrical it is reasonable to assume that the area supporting the npressive stress due to bending is equal to the area supporting the tensile stress due to bending, both as being symmetrically arranged about the original plastic neutral axis. Thus from Fig. 18.15(d) the uced plastic moment, $M_{P,R}$, is given by

$$M_{P,R} = \sigma_Y(Z_P - Z_a) \tag{18.20}$$

ere Z_a is the plastic section modulus for the area on which the axial load is assumed to act. From (18.6)

$$Z_a = \frac{2at_w}{2}\left(\frac{a}{2} + \frac{a}{2}\right) = a^2 t_w$$

)

$$P = 2at_w\sigma_Y$$

:hat

$$a = \frac{P}{2t_w\sigma_Y}$$

)stituting for Z_a, in Eq. (18.20) and then for a, we obtain

$$M_{P,R} = \sigma_Y\left(Z_P - \frac{P^2}{\quad}\right) \tag{18.21}$$

Let σ_a be the mean axial stress due to P taken over the complete area, A, of the beam section. Then

$$P = \sigma_a A$$

Substituting for P in Eq. (18.21)

$$M_{P,R} = \sigma_Y\left(Z_P - \frac{A^2}{4t_w}\frac{\sigma_a^2}{\sigma_Y^2}\right) \tag{18.22}$$

Thus the reduced plastic section modulus may be expressed in the form

$$Z_{P,R} = Z_P - Kn^2 \tag{18.23}$$

where K is a constant that depends upon the geometry of the beam section and n is the ratio of the mean axial stress to the yield stress of the material of the beam.

Equations (18.22) and (18.23) are applicable as long as the neutral axis lies in the web of the beam section. In the rare case when this is not so, reference should be made to advanced texts on structural steel design. In addition the design of beams carrying compressive loads is influenced by considerations of local and overall instability, as we shall see in Chapter 21.

EXAMPLE 18.8

If the propped cantilever of Ex. 18.7 is subjected to an axial load of 150 kN in addition to the 100 kN load at mid-span determine whether or not the selected Universal Beam is still adequate.

From Steel Tables the cross sectional area of the beam is 58.9 cm^2 and its web thickness is 6.9 mm. The mean axial stress is then

$$\sigma_a = \frac{150 \times 10^3}{58.9 \times 10^2} = 25.5 \text{ N/mm}^2$$

Then, from Eqs. (18.22) and (18.23) the reduced plastic section modulus is given by

$$Z_{P,R} = 886.3 - \frac{(58.9)^2}{4 \times (6.9/10)} \times \frac{25.5^2}{300^2}$$

which gives

$$Z_{P,R} = 877.2 \text{ cm}^3$$

The required plastic modulus of the beam section is 833.3 cm^3 so that the beam section is still adequate.

18.3 Plastic analysis of frames

The plastic analysis of frames is carried out in a very similar manner to that for beams in that possible collapse mechanisms are identified and the principle of virtual work used to determine the collapse loads. A complication does arise, however, in that frames, even though two-dimensional, can possess collapse mechanisms which involve both *beam* and *sway* mechanisms since, as we saw in Section 16.10 in the moment distribution analysis of portal frames, sway is produced by any asymmetry of the loading or frame.

EXAMPLE 18.9

Determine the value of the load W required to cause collapse of the frame shown in Fig. 18.16(a) if the plastic moment of all members of the frame is 200 kN m. Calculate also the support reactions at collapse.

We note that the frame and loading are unsymmetrical so that sway occurs. The bending moment diagram for the frame takes the form shown in Fig. 18.16(b) so that there are three possible collapse mechanisms as shown in Fig. 18.17.

In Fig. 18.17(a) the horizontal member BCD has collapsed with plastic hinges forming at B, C and D; this is termed a *beam mechanism.* In Fig. 18.17(b) the frame has swayed with hinges forming at A, B, D and E; this, for obvious reasons, is called a *sway mechanism.* Fig. 18.17(c) shows a *combined mechanism* which incorporates both the beam and sway mechanisms. However, in this case, the moments at B due to the vertical load at C and the horizontal load at B oppose each other so that the moment at B will be the smallest of the five peak moments and plastic hinges will form at

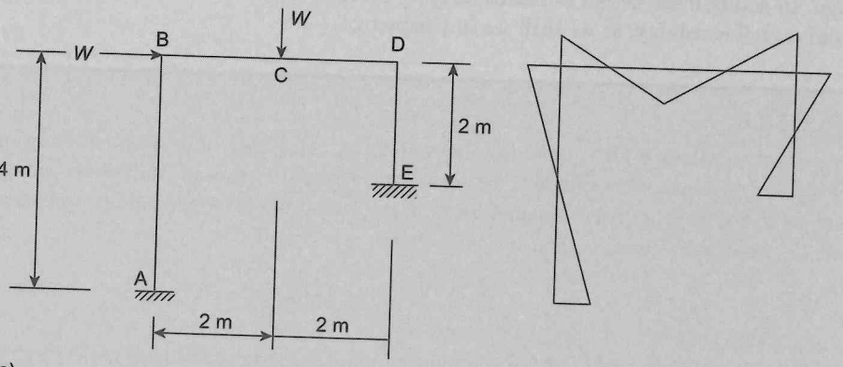

(a) (b)

FIGURE 18.16
Portal frame of Ex. 18.9.

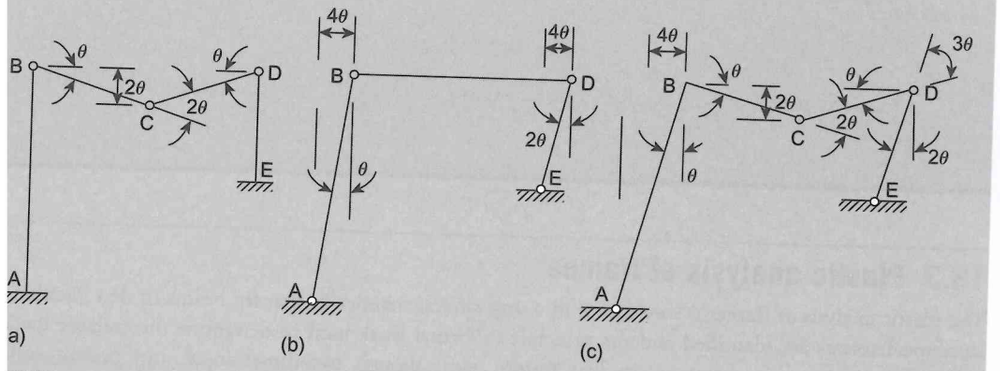

a) (b) (c)

IGURE 18.17
collapse mechanisms for the frame of Ex. 18.9.

the other locations. We say, therefore, that there is a *hinge cancellation* at B; the angle ABC then remains a right angle. We shall now examine each mechanism in turn to determine the value of W required to cause collapse. We shall designate the plastic moment of the frame as M_P.

Beam mechanism

Suppose that BC is given a small rotation θ. Since CD = CB then CD also rotates through the angle θ and the relative angle between CD and the extension of BC is 2θ. Then, from the principle of virtual work

$$W2\theta = M_P\theta + M_P2\theta + M_P\theta \tag{i}$$

which gives

$$W = 2M_P$$

In the virtual work equation 2θ is the vertical distance through which W moves and the first, second and third terms on the right hand side represent the internal work done by the plastic moments at B, C and D respectively.

Sway mechanism

The vertical member AB is given a small rotation θ, ED then rotates through 2θ. Again, from the principle of virtual work

$$W4\theta = M_P\theta + M_P\theta + M_P2\theta + M_P2\theta \tag{ii}$$

i.e.

$$W = \frac{3}{2}M_P$$

Combined mechanism

Since, now, there is no plastic hinge at B there is no plastic moment at B. Then, the principle of virtual work gives

$$W4\theta + W2\theta = M_P\theta + M_P2\theta + M_P3\theta + M_P2\theta \tag{iii}$$

from which

$$W = \frac{4}{3}M_P$$

We could have obtained Eq. (iii) directly by adding Eqs (i) and (ii) and anticipating the hinge cancellation at B. Eq. (i) would then be written

$$W2\theta = \{M_P\theta\} + M_P2\theta + M_P\theta \tag{iv}$$

where the term in curly brackets is the internal work done by the plastic moment at B. Similarly Eq. (ii) would be written

$$W4\theta = M_P\theta + \{M_P\theta\} + M_P2\theta + M_P2\theta \tag{v}$$

Adding Eqs (iv) and (v) and dropping the term in curly brackets gives

$$W6\theta = 8M_P\theta$$

as before.

From Eqs (i), (ii) and (iii) we see that the critical mechanism is the combined mechanism and ne lowest value of W is $4M_P/3$ so that

$$W = \frac{4 \times 200}{3}$$

e.

$$W = 266.7 \text{ kN}$$

igure 18.18 shows the support reactions corresponding to the collapse mode. The internal moment t D is M_P (D is a plastic hinge) so that, taking moments about D for the forces acting on the mem-er ED

$$R_{E,H} \times 2 = M_P = 200 \text{ kN m}$$

› that

$$R_{E,H} = 100 \text{ kN}$$

esolving horizontally

$$R_{A,H} + 266.7 - 100 = 0$$

om which

$$R_{A,H} = -166.7 \text{ kN} \quad \text{(to the left)}$$

aking moments about A

$$R_{E,V} \times 4 + R_{E,H} \times 2 - 266.7 \times 2 - 266.7 \times 4 = 0$$

hich gives

$$R_{E,V} = 350.1 \text{ kN}$$

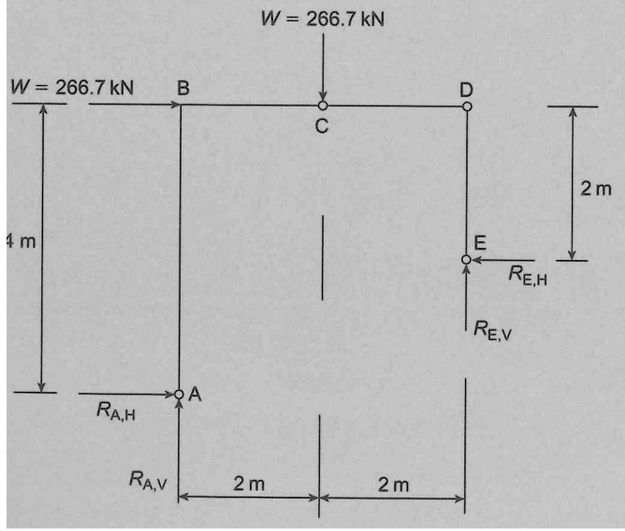

FIGURE 18.18
Support reactions at collapse in the frame of Ex. 18.9.

Finally, resolving vertically

$$R_{A,V} + R_{E,V} - 266.7 = 0$$

i.e.

$$R_{A,V} = -83.4 \text{ kN} \quad \text{(downwards)}$$

In the portal frame of Ex. 18.9 each member has the same plastic moment M_P. In cases where the members have different plastic moments a slightly different approach is necessary.

EXAMPLE 18.10

In the portal frame of Ex. 18.9 the plastic moment of the member BCD is $2M_P$. Calculate the critical value of the load W.

Since the vertical members are the weaker members plastic hinges will form at B in AB and at D in ED as shown, for all three possible collapse mechanisms, in Fig. 18.19. This has implications for the virtual work equation because in Fig. 18.19(a) the plastic moment at B and D is M_P while that at C is $2M_P$. The virtual work equation then becomes

$$W2\theta = M_P\theta + 2M_P2\theta + M_P\theta$$

which gives

$$W = 3M_P$$

For the sway mechanism

$$W4\theta = M_P\theta + M_P\theta + M_P2\theta + M_P2\theta$$

so that

$$W = \frac{3}{2}M_P$$

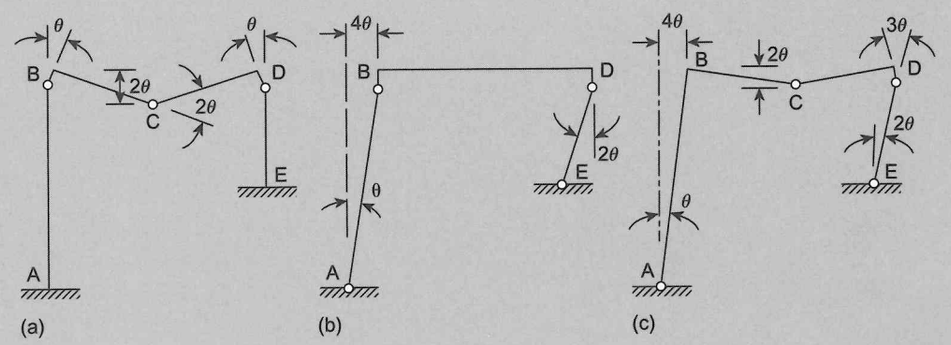

FIGURE 18.19
Collapse mechanisms for the frame of Ex. 18.10.

d for the combined mechanism

$$W4\theta + W2\theta = M_P\theta + 2M_P2\theta + M_P3\theta + M_P2\theta$$

om which

$$W = \frac{5}{3}M_P$$

Here we see that the minimum value of W which would cause collapse is $3M_P/2$ and that the ay mechanism is the critical mechanism.

We shall now examine a portal frame having a pitched roof in which the determination of displacements is more complicated.

XAMPLE 18.11

ne portal frame shown in Fig. 18.20(a) has members which have the same plastic moment M_P. etermine the minimum value of the load W required to cause collapse if the collapse mechanism is at shown in Fig. 18.20(b).

In Exs 18.9 and 18.10 the displacements of the joints of the frame were relatively simple to determine since all the members were perpendicular to each other. For a pitched roof frame the calculation is more difficult; one method is to use the concept of *instantaneous centres.*

In Fig. 18.21 the member BC is given a *small* rotation θ. Since θ is small C can be assumed to ove at right angles to BC to C′. Similarly the member DE rotates about E so that D moves horintally to D′. Further, since C moves at right angles to BC and D moves at right angles to DE it llows that CD rotates about the instantaneous centre, I, which is the point of intersection of BC d ED produced; the lines IC and ID then rotate through the same angle ϕ.

From the triangles BCC′ and ICC′

$$CC' = BC\theta = IC\phi$$

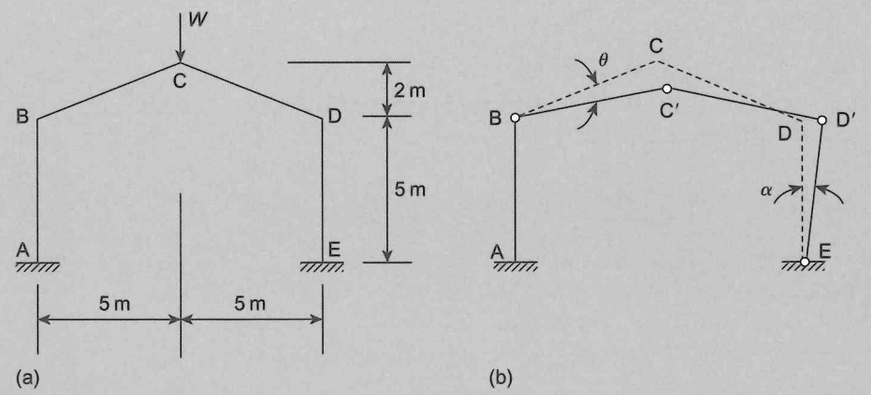

FIGURE 18.20
Collapse mechanism for the frame of Ex. 18.11.

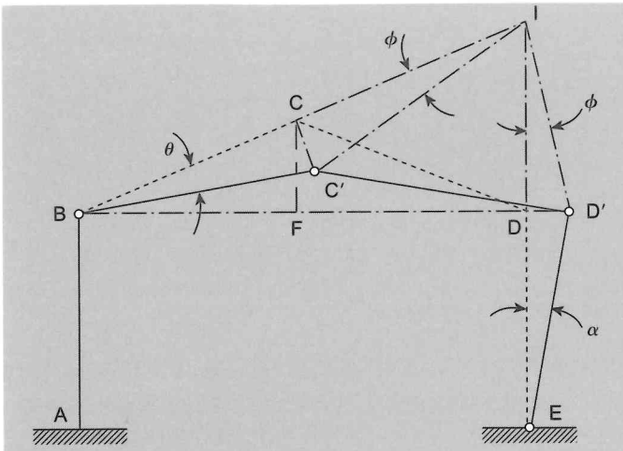

FIGURE 18.21
Method of instantaneous centres for the frame of Ex. 18.11.

so that

$$\phi = \frac{BC}{IC}\theta \qquad \text{(i)}$$

From the triangles EDD′ and IDD′

$$DD' = ED\alpha = ID\phi$$

Therefore

$$\alpha = \frac{ID}{ED}\phi = \frac{ID}{ED}\frac{BC}{IC}\theta \qquad \text{(ii)}$$

Now we drop a perpendicular from C to meet the horizontal through B and D at F. Then, from the similar triangles BCF and BID

$$\frac{BC}{CI} = \frac{BF}{FD} = \frac{5}{5} = 1$$

so that BC = CI and, from Eq. (i), $\phi = \theta$. Also

$$\frac{CF}{ID} = \frac{BF}{BD} = \frac{5}{10} = \frac{1}{2}$$

from which ID = 2CF = 4 m. Then, from Eq. (ii)

$$\alpha = \frac{4}{5}\theta$$

Finally, the vertical displacement of C to C′ is BFθ (=5θ).
The equation of virtual work is then

$$W5\theta = M_P\theta + M_P(\theta + \alpha) + M_P(\phi + \alpha) + M_P\alpha$$

Substituting for ϕ and α in terms of θ from the above gives

$$W = 1.12M_P$$

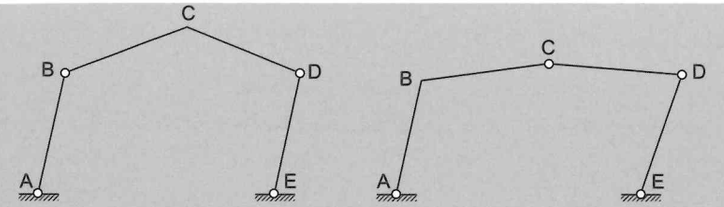

GURE 18.22

ossible collapse mechanisms for the frame of Ex. 18.11 with sway.

e failure mechanism shown in Fig. 18.20(b) does not involve sway. If, however, a horizontal load e applied at B, say, then sway would occur and other possible failure mechanisms would have to investigated; two such mechanisms are shown in Fig. 18.22. Note that in Fig. 18.22(a) there is a ge cancellation at C and in Fig. 18.22(b) there is a hinge cancellation at B. In determining the lapse loads of such frames the method of instantaneous centres still applies.

oads applied to frames are not always concentrated and may be distributed along one or more bers. To illustrate the method of analysis of such frames we shall consider the relatively simple e of Ex. 18.12.

AMPLE 18.12

e portal frame shown in Fig. 18.23(a) carries a uniformly distributed load of total value $4W$ across horizontal member BD in addition to a horizontal concentrated load of W at B. If the plastic ment of the member BD is $2M_P$ while that of the vertical columns is M_P determine the critical ue of the load W.

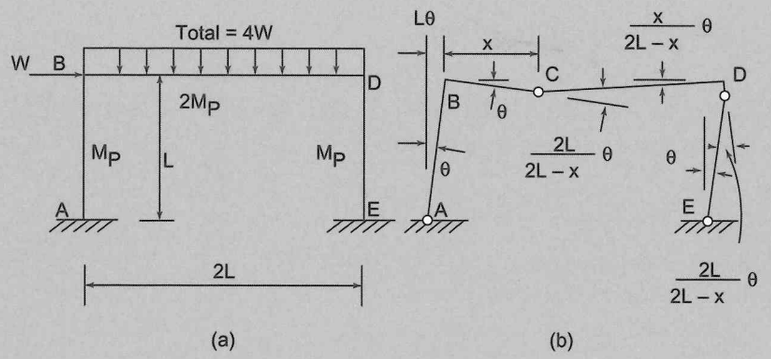

GURE 18.23

ame carrying a uniformly distributed load.

Since the columns are the weaker members plastic hinges will form at B in AB and at D in DE. However, as in Ex. 18.9, we can assume a hinge cancellation at B so that the collapse mechanism is that shown in Fig. 18.23(b). There will be a further hinge at C in BD where the bending moment is a maximum, a distance x, say, from B. The problem then is to determine the value of x.

Referring to Fig. 18.23(b) the principle of virtual work gives

$$M_P\theta + M_P\theta + M_P\left(\frac{2L}{2L-x}\right)\theta + 2M_P\left(\frac{2L}{2L-x}\right)\theta = WL\theta + \frac{4W}{2L}x.\frac{x}{2}\theta + \frac{4W}{2L}(2L-x)\left(\frac{2L-x}{2}\right)\left(\frac{x}{2L-x}\right)\theta$$

which simplifies to

$$M_P = W\frac{(2L^2 + 3Lx - 2x^2)}{10L - 2x} \qquad \text{(i)}$$

This will be a maximum when $dM_P/dx = 0$. Then, differentiating the above and equating to zero gives

$$4x^2 - 40Lx + 34L^2 = 0$$

the solution of which is

$$x = 0.94L$$

Substituting in Eq. (i) gives

$$M_P = 0.376WL$$

If it is assumed that the hinge in BD is midway along its length then the virtual work equation is

$$M_P\theta + M_P\theta + M_P2\theta + 2M_P2\theta = WL\theta + 2\times\frac{4W}{2L}\frac{L\theta}{2}$$

from which

$$M_P = 0.375WL$$

which differs from the accurately calculated value by 0.27%.

PROBLEMS

P.18.1 Determine the plastic moment and shape factor of a beam of solid circular cross section having a radius r and yield stress σ_Y.

Ans. $M_P = 1.33\sigma_Y r^3$, $f = 1.69$.

P.18.2 Determine the plastic moment and shape factor for a thin-walled box girder whose cross section has a breadth b, depth d and a constant wall thickness t. Calculate f for $b = 200$ mm, $d = 300$ mm.

Ans. $M_P = \sigma_Y td(2b + d)/2$, $f = 1.17$.

3.3 A beam having the cross section shown in Fig. P.18.3 is fabricated from mild steel which has a yield stress of 300 N/mm^2. Determine the plastic moment of the section and its shape factor.

Ans. 256.5 kN m, 1.52.

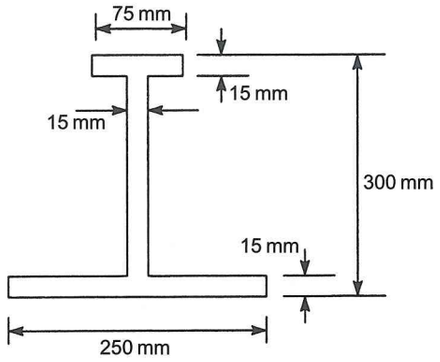

FIGURE P.18.3

3.4 A cantilever beam of length 6 m has an additional support at a distance of 2 m from its free end as shown in Fig. P.18.4. Determine the minimum value of W at which collapse occurs if the section of the beam is identical to that of Fig. P.18.3. State clearly the form of the collapse mechanism corresponding to this ultimate load.

Ans. 128.3 kN, plastic hinge at C.

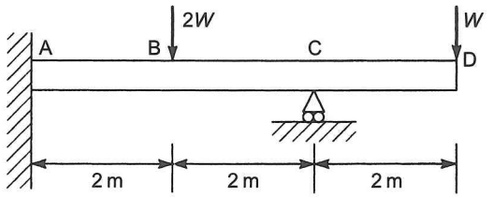

FIGURE P.18.4

3.5 A beam of length L is rigidly built-in at each end and carries a uniformly distributed load of intensity w along its complete span. Determine the ultimate strength of the beam in terms of the plastic moment, M_P, of its cross section.

Ans. $16M_P/L^2$.

3.6 A simply supported beam has a cantilever overhang and supports loads as shown in Fig. P.18.6. Determine the collapse load of the beam, stating the position of the corresponding plastic hinge.

Ans. $2M_P/L$, plastic hinge at D.

3.7 Determine the ultimate strength of the propped cantilever shown in Fig. P.18.7 and specify the corresponding collapse mechanism.

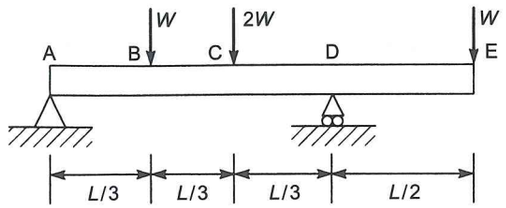

FIGURE P.18.6

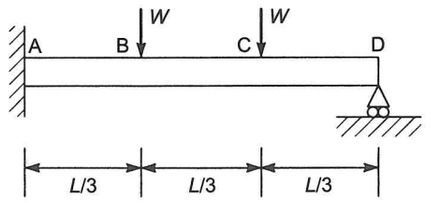

FIGURE P.18.7

P.18.8 The working loads, W, on the propped cantilever of Fig. P.18.7 are each 150 kN and its span is 6 m. If the yield stress of mild steel is 300 N/mm^2, suggest a suitable section for the beam using a load factor of 1.75 against collapse.

Ans. Universal Beam, 406 mm × 152 mm × 67 kg/m.

P.18.9 If the propped cantilever of Fig. P.18.7 is subjected to an axial load of 200 kN in addition to the two concentrated loads of 150 kN determine whether or not the beam section chosen in P.18.8 remains satisfactory.

Ans. Marginally satisfactory with no allowance for self-weight therefore use a UB 406 × 152 × 74 kg/m.

P.18.10 The members of a steel portal frame have the relative plastic moments shown in Fig. P.18.10. Calculate the required value of M for the ultimate loads shown.

Ans. 36.2 kN m.

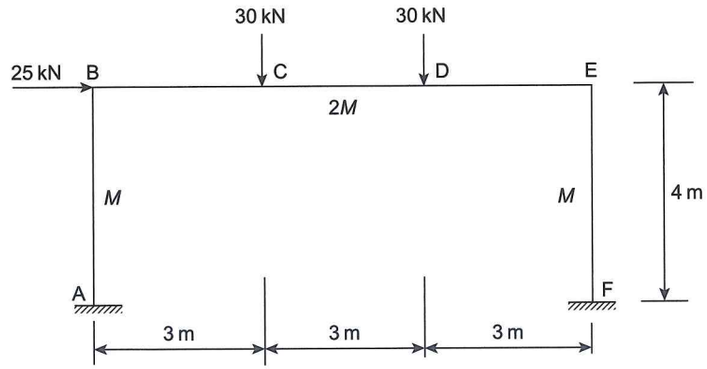

FIGURE P.18.10

11 The frame shown in Fig. P.18.11 is pinned to its foundation and has relative plastic moments of resistance as shown. If M has the value 108 kN m calculate the value of W that will just cause the frame to collapse.

Ans. 60 kN.

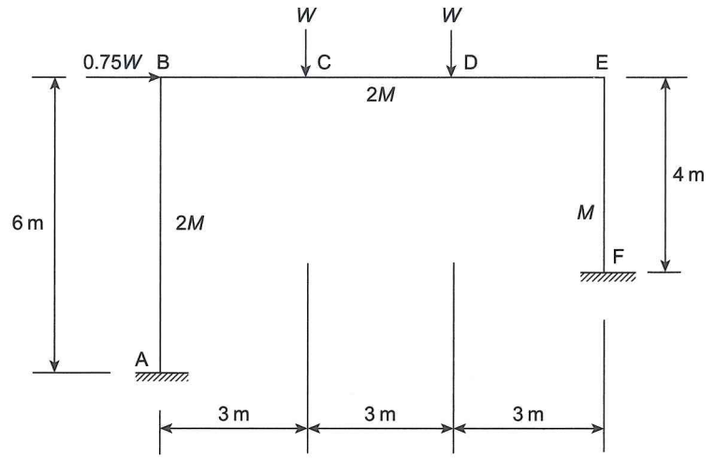

E P.18.11

12 Fig. P.18.12 shows a portal frame which is pinned to its foundation and which carries vertical and horizontal loads as shown. If the relative values of the plastic moments of resistance are those given determine the relationship between the load W and the plastic moment parameter M. Calculate also the foundation reactions at collapse.

Ans. $W = 0.3M$. Horizontal: $0.44W$ at A, $0.56W$ at G. Vertical: $0.89W$ at A, $2.11W$ at G.

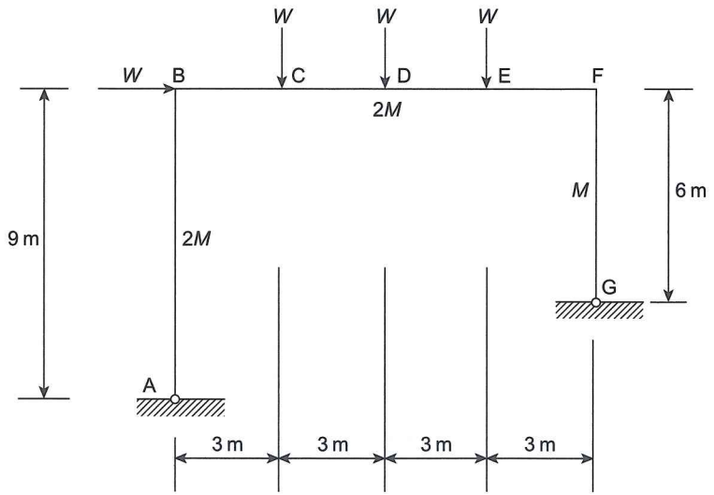

P.18.13 The steel frame shown in Fig. P.18.13 collapses under the loading shown. Calculate the value of the plastic moment parameter M if the relative plastic moments of resistance of the members are as shown. Calculate also the support reactions at collapse.

Ans. $M = 56$ kN m. Vertical: 32 kN at A, 48 kN at D. Horizontal: 13.3 kN at A, 33.3 kN at D.

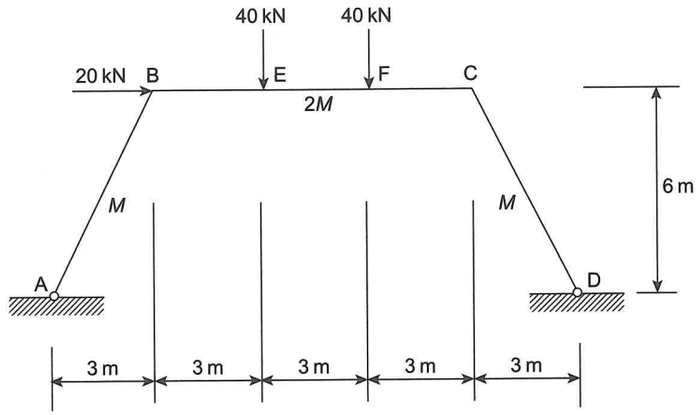

FIGURE P.18.13

P.18.14 The pitched roof portal frame shown in Fig. P.18.14 has columns with a plastic moment of resistance equal to M and rafters which have a plastic moment of resistance equal to $1.3M$. Calculate the smallest value of M that can be used so that the frame will not collapse under the given loading.

Ans. $M = 24$ kN m.

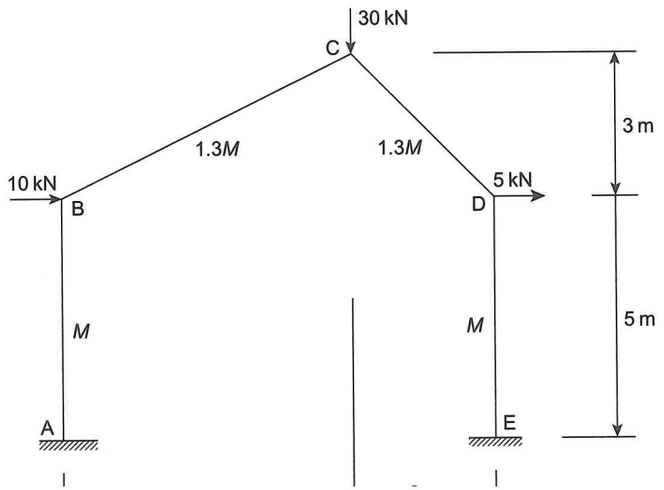

8.15 The frame shown in Fig. P.18.15 is pinned to the foundation at D and to a wall at A. The plastic moment of resistance of the column CD is 200 kN m while that of the rafters AB and BC is 240 kN m. For the loading shown calculate the value of P at which collapse will take place.

Ans. $P = 106.3$ kN.

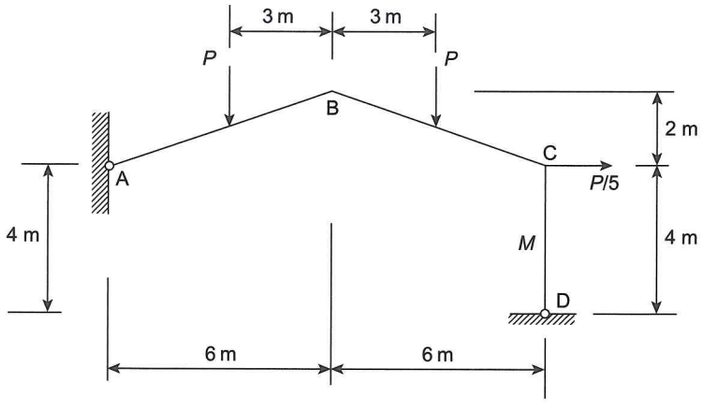

JRE P.18.15

8.16 The steel portal frame shown in Fig. P.18.16 is pinned to its foundations at A and E and the plastic moment of resistance of all the members of the frame is the same. If the frame is on the point of collapse under the loading shown calculate the actual plastic moment of resistance. Sketch the bending moment diagram of the frame at the onset of collapse giving the value of the bending moment at each joint.

Ans. $M_P = 47.83$ kN m. $M_B = 27.15$ kN m. $M_C = 21.57$ kN m, $M_D = 47.83$ kN m.

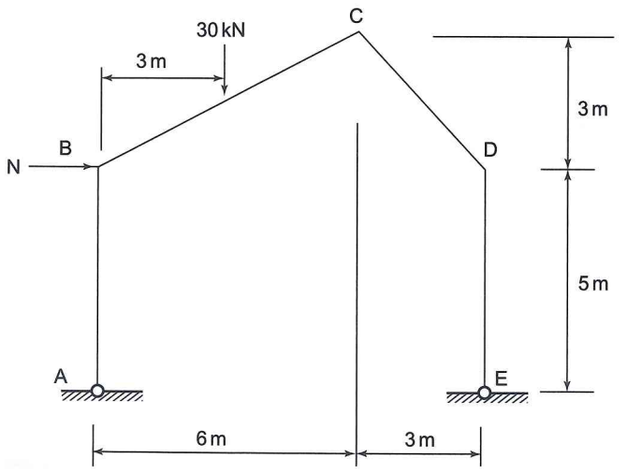

FIGURE P.18.16

P.18.17 If the vertical load W applied to the frame of Fig. 18.16(a) is increased to $4W$, is uniformly distributed along the member BD and the horizontal concentrated load W remains in position at B determine the value of W required to cause collapse. Assume that the plastic hinge in BD still occurs at C, the mid-point of BD.

Ans. $M_P = W$ (both the sway and combined mechanisms produce the same value).

P.18.18 Repeat P.18.17 but consider the more accurate positioning of the plastic hinge in BD. Comment on the result obtained.

Ans. $M_P = 1.125W$ (combined mechanism). See Solutions Manual for comment.

CHAPTER

eld Line Analysis of Slabs 19

theory presented in this chapter extends the ultimate load analysis of structures, begun in pter 18 for beams and frames, to reinforced concrete slabs.
tructural engineers, before the development of ultimate load analysis, designed reinforced concrete using elastic plate theory. This approach, however, gives no indication of the ultimate load-ring capacity of a slab and further analysis had to be carried out to determine this condition. rnatively, designers would use standard tables of bending moment distributions in orthogonal plates different support conditions. These standard tables were presented, for reinforced concrete slabs, odes of Practice but were restricted to rectangular slabs which, fortunately, predominate in rein-d concrete construction. However, for non-rectangular slabs and slabs with openings, these s cannot be used so that other methods are required. The method presented here, *yield line theory*, developed in the early 1960s by the Danish engineer, K.W. Johansen.

1 Yield line theory

e are two approaches to the calculation of the ultimate load-carrying capacity of a reinforced con-slab involving yield line theory. One is an energy method which uses the principle of virtual work the other, an equilibrium method, studies the equilibrium of the various parts of the slab formed ıe yield lines; we shall restrict the analysis to the use of the principle of virtual work since this was ed in Chapter 18 to the calculation of collapse loads of beams and frames.

d lines

ıb is assumed to collapse at its ultimate load through a system of nearly straight lines which are l *yield lines*. These yield lines divide the slab into a number of *panels* and this pattern of yield lines panels is termed the *collapse mechanism*; a typical collapse mechanism for a simply supported ngular slab carrying a uniformly distributed load is shown in Fig. 19.1(a).
he panels formed by the supports and yield lines are assumed to be plane (at fracture elastic defor-ons are small compared with plastic deformations and are ignored) and therefore must possess a ıetric compatibility; the section AA in Fig. 19.1(b) shows a cross section of the collapsed slab. It is er assumed that the bending moment along all yield lines is constant and equal to the value corre-ding to the yielding of the steel reinforcement. Also, the panels rotate about axes along the sup-d edges and, in a slab supported on columns, the axes of rotation pass through the columns, see 19.2(b). Finally, the yield lines on the sides of two adjacent panels pass through the point of inter-ın of their axes of rotation. Examples of yield line patterns are shown in Fig. 19.2. Note the con-ons for the representation of different support conditions.
ı the collapse mechanisms of Figs 19.1(a) and 19.2(b) the supports are simple supports so that the s free to rotate along its supported edges. In Fig. 19.2(a) the left-hand edge of the slab is built in

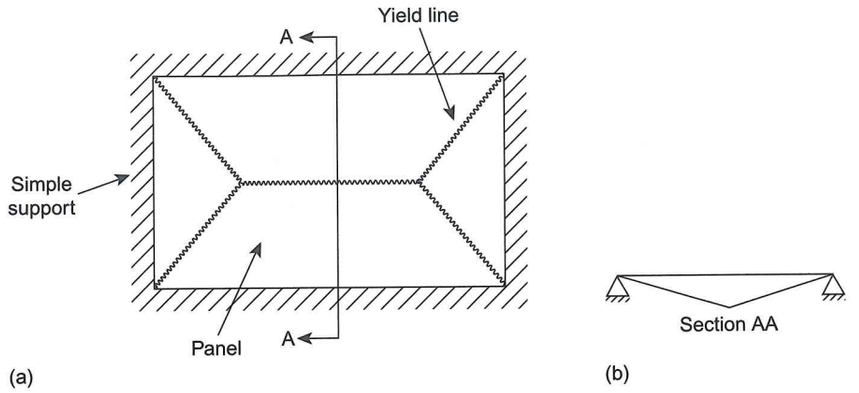

FIGURE 19.1
Collapse mechanism for a rectangular slab.

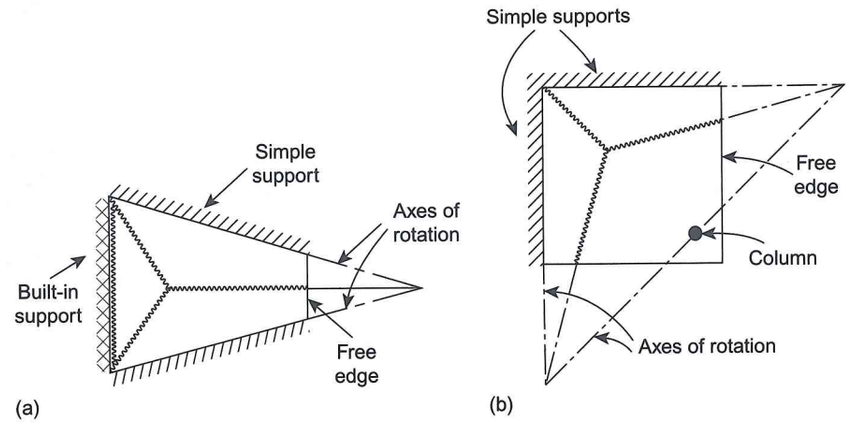

FIGURE 19.2
Collapse mechanisms and diagrammatic representation of support conditions.

and not free to rotate. At collapse, therefore, a yield line will develop along this edge as shown. Along this yield line the bending moment will be hogging, i.e. negative, and the reinforcing steel will be positioned in the upper region of the slab; where the bending moment is sagging the reinforcing steel will be positioned in the lower region.

Ultimate moment along a yield line

Figure 19.3(a) shows a portion of a slab reinforced in two directions at right angles; the ultimate moments of resistance of the reinforcement are m_1 per unit width of slab and m_2 per unit width of

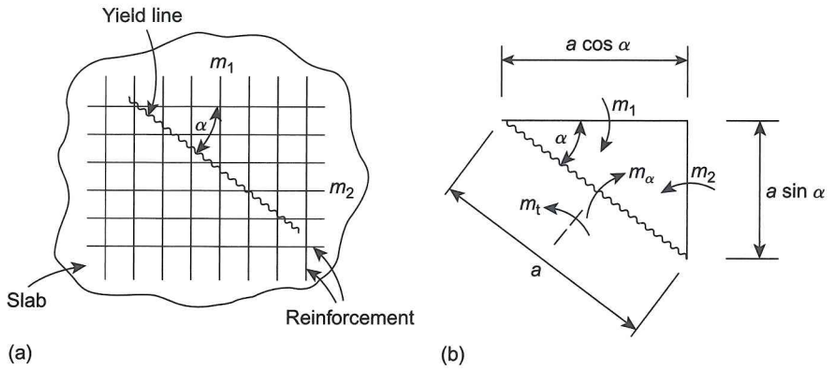

RE 19.3

rmination of the ultimate moment along a yield line.

gular element formed by a length a of the yield line and the reinforcement as shown in Fig. 19.3(b). ıı, from the moment equilibrium of the element in the direction of m_α, we have

$$m_\alpha a = m_1 a \cos\alpha(\cos\alpha) + m_2 a \sin\alpha(\sin\alpha)$$

$$m_\alpha = m_1 \cos^2\alpha + m_2 \sin^2\alpha \tag{19.1}$$

Now, from the moment equilibrium of the element in the direction of m_t

$$m_t a = m_1 a \cos\alpha(\sin\alpha) - m_2 a \sin\alpha(\cos\alpha)$$

ıat

$$m_t = \frac{(m_1 - m_2)}{2} \sin 2\alpha \tag{19.2}$$

Note that for an isotropic slab, which is one equally reinforced in two perpendicular directions, $m_2 = m$, say, so that

$$m_\alpha = m \quad m_t = 0 \tag{19.3}$$

rnal virtual work due to an ultimate moment

re 19.4 shows part of a slab and its axis of rotation. Let us suppose that at some point in the slab is a known yield line inclined at an angle α to the axis of rotation; the ultimate moment is m per length along the yield line. Let us further suppose that the slab is given a small virtual rotation θ. virtual work done by the ultimate moment is then given by

$$VW(m) = (mL)(\cos\alpha)\theta = m(L\cos\alpha)\theta \tag{19.4}$$

We see, therefore, from Eq. (19.4), that the internal virtual work done by an ultimate moment g a yield line is the value of the moment multiplied by the angle of rotation of the slab and the

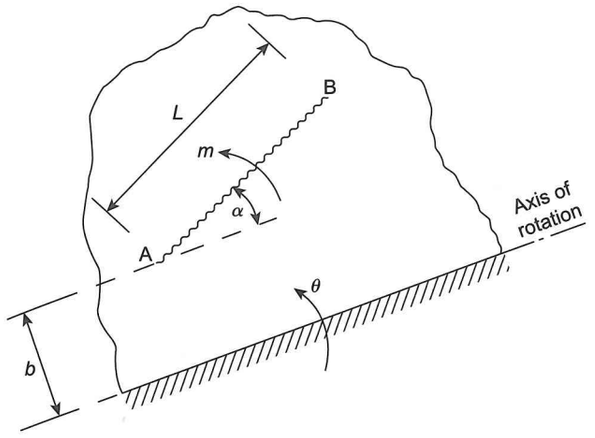

FIGURE 19.4

Determination of the work done by an ultimate moment.

Usually, rather than give a panel of a slab a virtual rotation, it is simpler to give a point on a yield line a unit virtual displacement. If, in Fig. 19.4 for example, the point A is given a unit virtual displacement then

$$\theta = \frac{1}{b}$$

where b is the perpendicular distance of A from the axis of rotation. Clearly the displacement of B due to θ would be greater than unity.

Virtual work due to an applied load

For a slab subjected to a distributed load of intensity $w(x, y)$ the virtual work done by the load corresponding to the virtual rotation of the slab panels is given by

$$VW(w) = \int\int wu \, dx \, dy \tag{19.5}$$

where u is the virtual displacement at any point (x, y).

Conveniently, many applied loads on slabs are uniformly distributed so that we may calculate the total load on a slab panel and then determine the displacement of its centroid in terms of the given virtual displacement; the virtual work done by the load is then the product of the two and the total virtual work is the sum of the virtual works from each panel.

Having obtained the virtual work corresponding to the internal ultimate moments and the virtual work due to the applied load then the principle of virtual work gives

$$VW(w) = VW(m) \tag{19.6}$$

which gives the ultimate load applied to the slab in terms of its ultimate moment of resistance. This means, in fact, that we can calculate the required moment of resistance for a slab which supports a given load or, alternatively, we can obtain the maximum load that can be applied to a slab having a known moment of resistance. In the former case the given, or working, load is multiplied by a load factor to obtain an ultimate load while in the latter case the ultimate load is divided by the load factor.

The yield line pattern assumed for the collapse mechanism in a slab may not, of course, be the true pattern so that, as for the plastic analysis of beams and frames, the virtual work equation (Eq. (19.6))

refore, for a given ultimate load (actual load × load factor), the calculated required ultimate nent of resistance is either correct or less than it should be. In other words, the solution is either ect or unsafe so that the virtual work approach gives an upper bound on the carrying capacity of slab. Generally, in design, two or more yield line patterns are assumed and the maximum value of ultimate moment of resistance obtained.

XAMPLE 19.1

ıe slab shown in Fig. 19.5 is isotropically reinforced and is required to carry an ultimate design ıd of 12 kN/m^2. If the ultimate moment of resistance of the reinforcement is m per unit width of b in the direction shown, calculate the value of m for the given yield line pattern.

We note that the slab is simply supported on three sides and is free on the other. Suppose that e junction c of the yield lines is given a unit virtual displacement.

Then

$$\theta_A = \frac{1}{x}\theta_B = \theta_C = \frac{1}{2}$$

The internal virtual work is therefore given by

$$VW(m) = m \times 4\frac{1}{x} + 2\,m \times 4\frac{1}{2} \qquad \text{(i)}$$

The first term on the right-hand side of Eq. (i) is the work done by the ultimate moment on the ıgonal yield lines ac and bc on the boundary of panel A and is obtained as follows. We have seen ıt, for an isotropic slab, the ultimate moment along an inclined yield line is equal to the moment

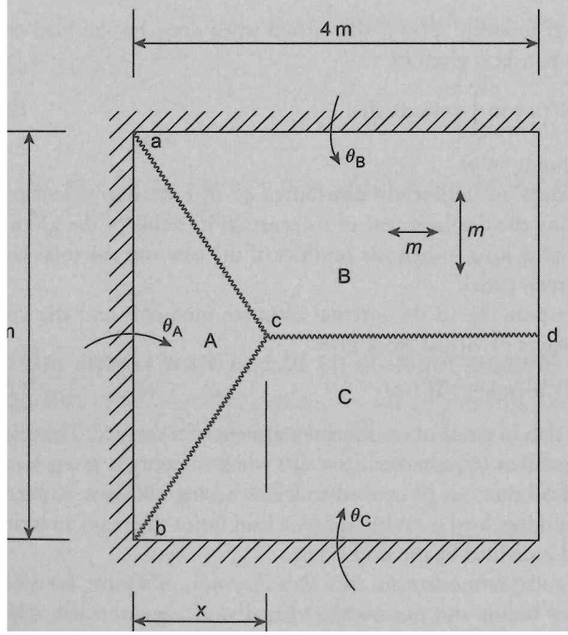

FIGURE 19.5

of resistance of the reinforcement irrespective of the inclination of the reinforcement to the yield line (Eq. (19.3)). Further, the work done by the ultimate moment on an inclined yield line is the product of the moment, the projection of the yield line on the axis of rotation and the angle of rotation of the panel (Eq. (19.4)). The second term on the right-hand side of Eq. (i) represents the work done by the ultimate moment on the diagonal and horizontal yield lines bordering each of the panels B and C; from symmetry the contribution of both panels will be the same. From the above argument and considering panel B

$$VW(m)_B = mx\left(\frac{1}{2}\right) + m(4-x)\left(\frac{1}{2}\right) = 4\,m\left(\frac{1}{2}\right)$$

Similarly for panel C.

Equation (i) simplifies to

$$VW(m) = 4\,m\left(\frac{1}{x} + 1\right) \qquad \text{(ii)}$$

The work done by the applied load is most easily found by dividing each of the panels B and C into a rectangle and a triangle, panel A is a triangle. Then

$$VW(w) = 12\left\{\frac{1}{2} \times 4x \times \frac{1}{3} + 2\left[\frac{1}{2}x \times 2 \times \frac{1}{3} + (4-x) \times 2 \times \frac{1}{2}\right]\right\} \qquad \text{(iii)}$$

In Eq. (iii) the displacement of the centroids of the triangles in panels A, B and C is 1/3 while the displacement of the centroids of the rectangular portions of panels B and C is 1/2. Eq. (iii) simplifies to

$$VW(w) = 96 - 8x \qquad \text{(iv)}$$

Equating Eqs (ii) and (iv)

$$4m\left(\frac{1}{x} + 1\right) = 96 - 8x$$

from which

$$m = 2\left(\frac{12x - x^2}{1+x}\right) \qquad \text{(v)}$$

For a maximum, $(dm/dx) = 0$, i.e.

$$0 = \frac{(1+x)(12-2x) - (12x - x^2)}{(1+x)^2}$$

which reduces to

$$x^2 + 2x - 12 = 0$$

from which

$$x = 2.6 \text{ m (the negative root is ignored)}$$

Then, from Eq. (v)

$$m = 13.6 \text{ kNm/m}$$

n some cases the relationship between the ultimate moment m and the dimension x is complex so the determination of the maximum value of m by differentiation is tedious. A simpler approach ld be to adopt a trial and error method in which a series of values of x are chosen and then m plot- against x.

n the above we have calculated the internal virtual work produced by an ultimate moment of resis- e which acts along a yield line (Fig. 19.4). This situation would occur if the direction of the rein- ement was perpendicular to the direction of the yield line or if the reinforcement was isotropic (see (19.3)). A more complicated case arises when a band of reinforcement is inclined at an angle to a l line and the slab is not isotropic.

Consider the part of a slab shown in Fig. 19.6 in which the yield line AB is of length L and is ned at an angle α to the axis of rotation. Suppose also that the direction of the reinforcement m is n angle β to the normal to the yield line.

Then, if the point B is given a unit virtual displacement perpendicular to the plane of the slab the e of rotation θ is given by

$$\theta = \frac{1}{b}$$

re b is the perpendicular distance of B from the axis of rotation. Further, the rotation θ_r of the slab plane parallel to the reinforcement is given by

$$\theta_r = \frac{1}{r}$$

re r is the distance of B from the axis of rotation in a direction parallel to the reinforcement.

From the above

$$\theta_r = \theta\frac{b}{r} \tag{19.7}$$

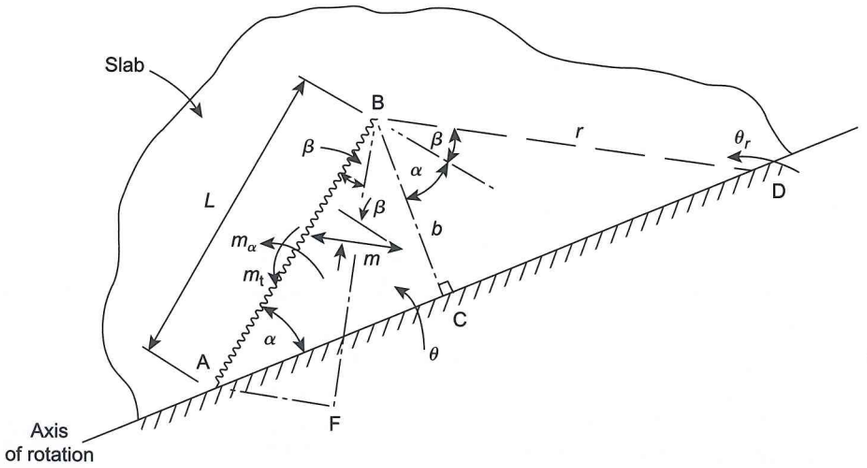

RE 19.6

Also, from triangle BCD

$$\frac{b}{r} = \cos(\alpha + \beta)$$

Then, from Eq. (19.7)

$$\theta_r = \theta\ \cos(\alpha + \beta) \tag{19.8}$$

Now, from Eq. (19.1) in which, in this case, $m_1 = m$, $m_2 = 0$ and $\alpha = \beta$

$$m_\alpha = m\ \cos^2\beta \tag{19.9}$$

and

$$m_t = \left(\frac{m}{2}\right)\sin 2\beta \tag{19.10}$$

The internal virtual work due to the rotation θ is given by

$$VW(m) = (m_\alpha L)(\cos\alpha)\theta - (m_t L)(\sin\alpha)\theta \tag{19.11}$$

where the component of $(m_t L)$ perpendicular to the axis of rotation opposes the component of $(m_\alpha L)$. Substituting in Eq. (19.11) for m_α and m_t from Eqs (19.9) and (19.10), respectively we have

$$VW(m) = (mL\cos^2\beta)(\cos\alpha)\theta - \left[\left(\frac{m}{2}\right)L\sin 2\beta\right](\sin\alpha)\theta$$

which simplifies to

$$VW(m) = m(L\cos\beta)\theta(\cos\beta\cos\alpha - \sin\beta\sin\alpha)$$

or

$$VW(m) = m(L\cos\beta)\theta\cos(\alpha + \beta) \tag{19.12}$$

Substituting for $\theta\cos(\alpha + \beta)$ from Eq. (19.8) gives

$$VW(m) = m(L\cos\beta)\theta_r \tag{19.13}$$

In Eq. (19.13) the term $L\cos\beta$ is the projection BF of the yield line AB on a line perpendicular to the direction of the reinforcement. Equation (19.13) may be written as

$$VW(m) = m(L\cos\beta)\frac{1}{r} \tag{19.14}$$

where, as we have seen, r is the radius of rotation of the slab in a plane parallel to the direction of the reinforcement.

EXAMPLE 19.2

Determine the required moment parameter m for the slab shown in Fig. 19.7 for an ultimate load of 10 kN/m^2; the relative values of the reinforcement are as shown.

Note that in Fig. 19.7 the reinforcement of 1.2 m resists a hogging bending moment at the built-in edge of the slab and is shown dotted.

The first step is to choose a yield line pattern. We shall assume the collapse mechanism shown in Fig. 19.8; in practice a number of different patterns might be selected and investigated. Note that

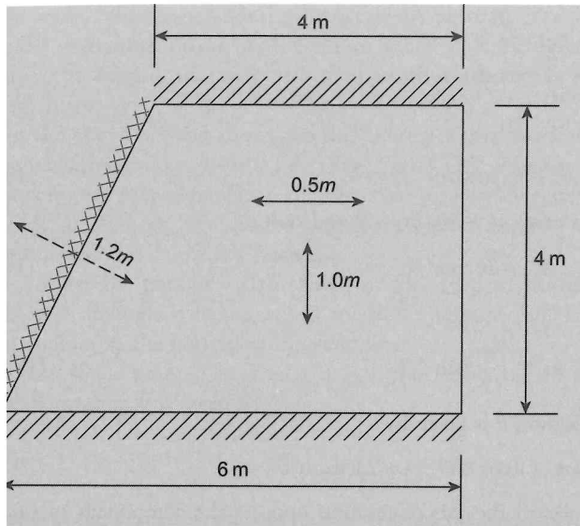

FIGURE 19.7
Slab of Ex. 19.2.

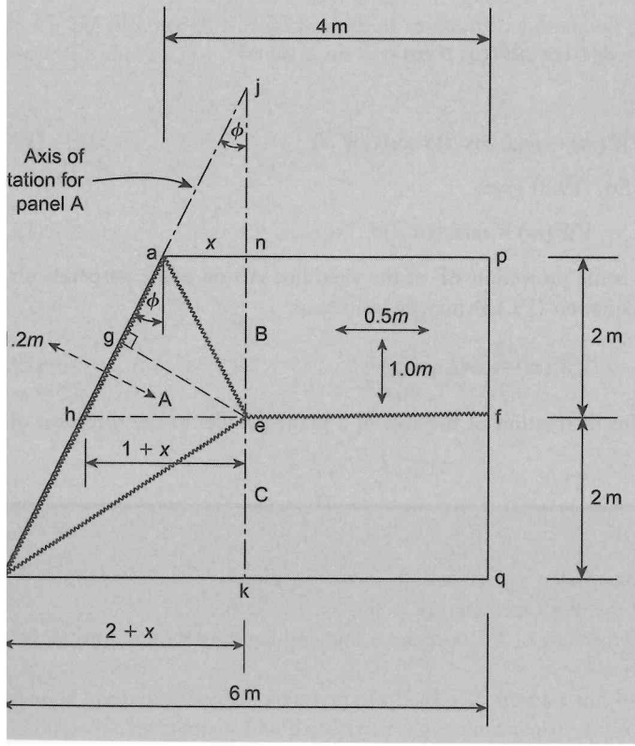

FIGURE 19.8
Yield line pattern for the slab of Ex. 19.2.

there will be a yield line ad along the built-in edge. Suppose, now, that we impose a unit virtual displacement on the yield line at f; e will suffer the same virtual displacement since ef and ab are parallel. The angle of rotation of the panel B (and C) is then 1/2. Panel A rotates about the line ad and its angle of rotation is 1/ge where ge is the perpendicular distance of ad from e. From the dimensions given ad = 4.5 m and ge = he cos $\phi = (1 + x)(4/4.5) = 0.89(1 + x)$.

The slab is not isotropic so that we shall employ the result of Eq. (19.14) to determine the internal virtual work due to the ultimate moments in the different parts of the slab. Therefore, for each yield line we need to determine its projection on a line perpendicular to the reinforcement and the corresponding radius of rotation. We shall adopt a methodical approach.

(1) Panel A

- Reinforcement 1.2 m

  The axis of rotation is the line ad and since the reinforcement is perpendicular to the yield line ad the projected length is ad = 4.5 m. The radius of rotation is ge = $0.89(1 + x)$. The virtual work is then

$$1.2\ m \times 4.5\left[\frac{1}{0.89(1+x)}\right] \tag{i}$$

- Reinforcement 0.5 m

  The sum of the projected length of the yield lines de and ea parallel to the reinforcement is 4 m and the radius of rotation is he = $1 + x$. The virtual work is then

$$0.5\ m \times 4\left[\frac{1}{(1+x)}\right] \tag{ii}$$

- Reinforcement 1.0 m

  The projection of the yield line de in a direction parallel to the reinforcement is dk = $2 + x$ and the corresponding radius of rotation is ej = he/tan $\phi = 2(1 + x)$.

  For the yield line ea the projected length is na = x and its radius of rotation is the same as that of the yield line de, i.e. $2(1 + x)$. However, since the centre of rotation is at j the displacement of the reinforcement crossing the yield line ea is less than its displacement as it crosses the yield line de. At de, therefore, the reinforcement will be sagging while at ea it will be hogging. The contributions to the virtual work at these two points will therefore be of opposite sign. The virtual work is then

$$\frac{1.0\ m[(2+x)-x]}{2(1+x)} = \frac{1.0\ m}{(1+x)} \tag{iii}$$

(2) Panel B

- Reinforcement 1.0 m

  We note that the 0.5 m reinforcement is parallel to the axis of rotation and does not, therefore, contribute to the virtual work in this panel. The projection of the yield lines ae and ef is 4 m and the radius of rotation is 2 m. The virtual work is then

$$1.0\ m \times \frac{4}{2} = 2.0\ m \tag{iv}$$

(3) Panel C

- Reinforcement 1.0 m

The situation in panel C is identical to that in panel B except that the projection of the yield lines de and ef is 6 m. The virtual work is then

$$3.0\,m \tag{v}$$

Adding the results of Eqs (i)–(v) we obtain the total internal virtual work, i.e.

$$VW(m) = \left(\frac{14.07 + 5x}{1 + x}\right) \tag{vi}$$

The external virtual work may be found by dividing the slab into rectangles enpf and ekqf and triangles ane, ekd and ade. Since the displacement of e is unity the displacement of each of the centroids of the rectangles will be 1/2 and the displacement of each of the centroids of the triangles will be 1/3. The total virtual work due to the applied load is then given by

$$VW(w) = 10\left[2(4-x)\left(\frac{2}{2}\right) + \left(\frac{x}{2}\right)\left(\frac{2}{3}\right) + 2(2+x)\left(\frac{1}{2}\right)\left(\frac{1}{3}\right) + 4.5 \times 0.89(1+x)\left(\frac{1}{2}\right)\left(\frac{1}{3}\right)\right]$$

which simplifies to

$$VW(w) = 10(9.33 - 0.67x) \tag{vii}$$

Equating internal and external virtual works, Eqs (vi) and (vii), we have

$$m = \frac{10(1+x)(9.33 - 0.67x)}{14.07 + 5x} \tag{viii}$$

The value of x corresponding to the maximum value of m may be found by differentiating Eq. (viii) with respect to x and equating to zero. Alternatively, a series of trial values of x may be substituted in Eq. (viii) and the maximum value of m obtained. Using the former approach gives $x = 2.71$ m from which

$$m = 10.9 \text{ kNm/m}$$

XAMPLE 19.3

ıe slab shown in Fig. 19.9(a) has an opening at the corner A to allow the passage of a hoist. The b is built in on the sides AB, BC and AD and is simply supported on the side DC. The relative lues of the moments of resistance per unit width for hogging and sagging bending at relevant posi-ns in the slab are shown in Fig. 19.9(b). For the typical yield line pattern shown in Fig. 19.9(a) lculate the value of the moment parameter m if the slab has to carry an ultimate design load of kN/m^2.

The rotations of the different parts of the slab are shown in Fig. 19.10.

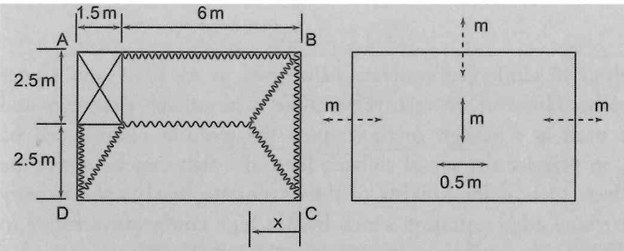

FIGURE 19.9
Slab of Ex. 19.3

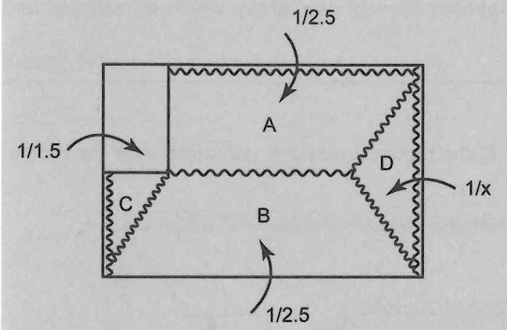

FIGURE 19.10
Rotations for slab of Ex. 19.4

The work absorbed by the different parts of the slab is as follows.

A: $(m + m) \times 6 \times (1/2.5) = 4.8\,m$
B: $m \times 7.5 \times (1/2.5) = 3\,m$
C: $(m + 0.5\,m) \times 2.5 \times (1/1.5) = 2.5\,m$
D: $(m + 0.5\,m) \times 5 \times (1/x) = 7.5\,m/x$

The total work absorbed is therefore $m[10.3 + (7.5/x)]$

The total work done by the load is:

$$12\left[2.5 \times 1.5 \times (1/3) + 5 \times x \times (1/3) + (6 - x) \times 5 \times (1/2)\right] = 195 - 10x$$

Equating the work absorbed by the slab to the work done by the load gives

$$m = \frac{195x - 10x^2}{10.3x + 7.5} \tag{i}$$

Differentiating Eq. (i) and equating to zero gives

$$x^2 + 1.456x - 14.199 = 0$$

the solution of which is

$$x = 3.11 \text{ m}$$

Substituting this value in Eq. (i) gives

$$m = 12.9 \text{ kNm/m}$$

2 Discussion

method presented here for the analysis of reinforced concrete slabs gives, as we have seen, upper d values for the collapse loads of slabs. However, in relatively simple cases of slab geometry and ng, the yield line method can be used as a design method since the fracture pattern can be ned with reasonable accuracy. Also, in practice the actual collapse load of a slab may be above the ated value because of secondary effects such as the kinking of the reinforcing steel in the vicinity e fracture line and the effect of horizontal edge restraints which induce high compressive forces in lane of the slab with a consequent increase in load capacity.

n alternative to yield line theory is the *strip method* proposed by A. Hillerborg at Stockholm in . This method is a direct design procedure as opposed to yield line theory which is analytical and fore will not be investigated here.

BLEMS

1 Determine, for the slab shown in Fig. P.19.1, the required moment parameter m if the design ultimate load is 14 kN/m^2.

Ans. 24.31 kNm/m.

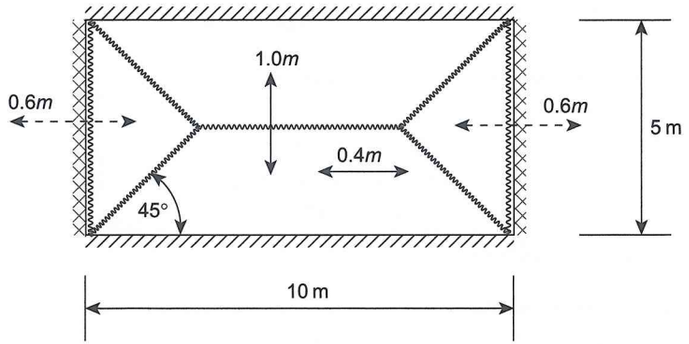

E P.19.1

2 The reinforced concrete slab shown in Fig. P.19.2(a) is designed to have an ultimate load capacity of 10 kN/m^2 across its complete area. Determine the required value of the moment parameter m given that the yield line pattern is as shown.

If an opening is introduced as shown in Fig. P.19.2(b) determine the corresponding required value of the moment parameter m.

Ans. 32.37 kNm/m, 35.27 kNm/m.

3 In the slab shown in Fig. P.19.3 Area 1 carries an ultimate load of intensity 12 kN/m^2 while Area 2 carries an ultimate load of intensity 8 kN/m^2. Determine the value of the moment parameter m assuming the yield line pattern shown.

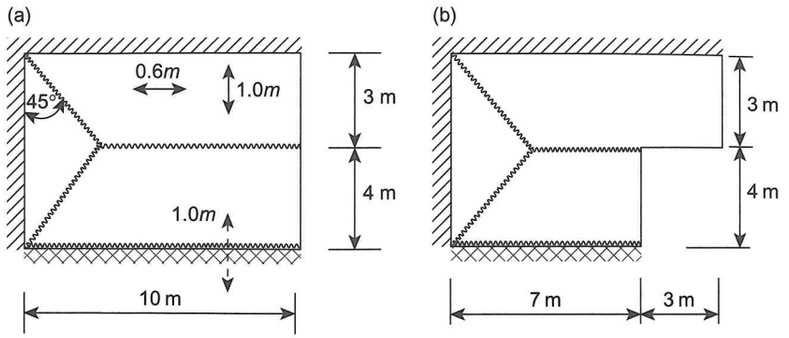

FIGURE P.19.2

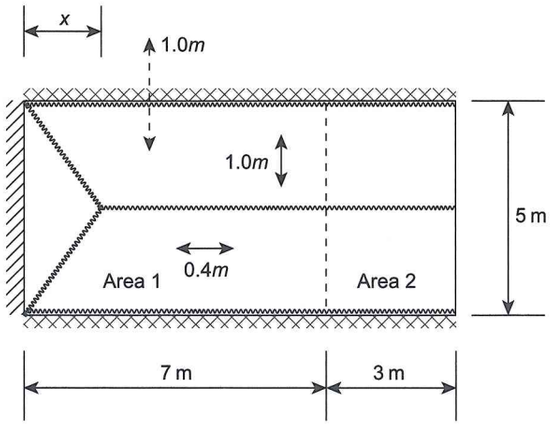

FIGURE P.19.3

P.19.4 Calculate the intensity of uniformly distributed load that would cause the reinforced concrete slab shown in Fig. P.19.4 to collapse given the yield line pattern shown.

Ans. 15.45 kN/m^2.

P.19.5 The reinforced concrete slab shown in Fig. P.19.5 is to be designed to carry an ultimate load of 15 kN/m^2. The distribution of reinforcement is to be such that the ultimate moments of resistance per unit width of slab for sagging bending are isotropic and of value m while the ultimate moment of resistance per unit width at continuous edges is 1.2 m. For the yield line pattern shown derive the general work equation and estimate the value of m by using trial values of $x = 2.0$, 2.5 and 3.0 m.

Ans. 9.70 kNm/m.

P.19.6 The reinforced concrete slab shown in Fig. P.19.6 is reinforced such that the sagging moments of resistance are isotropic and of value 1.0 m while the hogging moment of resistance at all built-in edges is 1.4 m. Estimate the required value of the moment parameter m if the ultimate design load intensity is 20 kN/m^2.

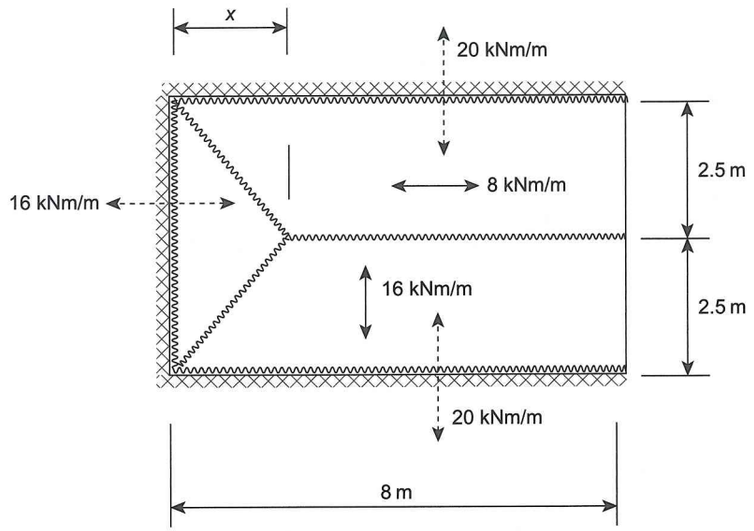

RE P.19.4

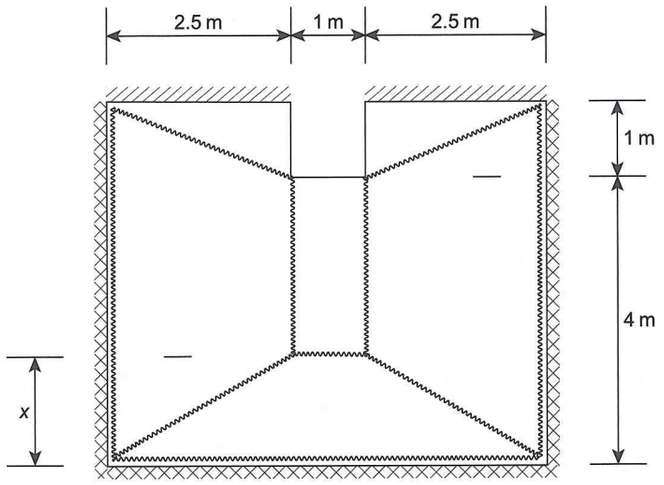

FIGURE P.19.5

.7 The reinforced concrete slab shown in Fig. P.19.7(a) is simply supported on the sides AB and DC and is built in on the sides AC and BC. The layout of reinforcement is such that the sagging moments of resistance about the x and y axes are 1.0 m and 0.4 m per unit width respectively while the hogging moment of resistance about the y direction at the built in edges is 0.6 m per unit width. If the design ultimate load is 14 kN/m^2 determine the required moment parameter m of the resistance of the slab. By consideration of the secondary yield line

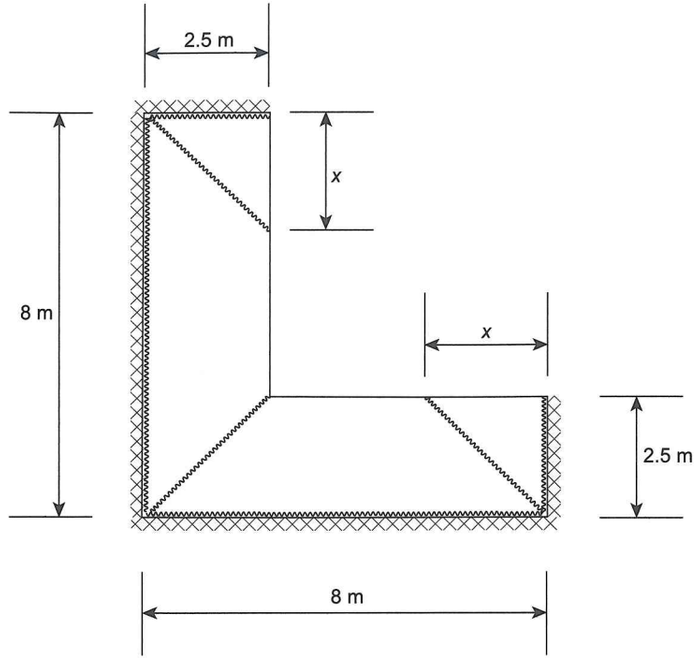

FIGURE P.19.6

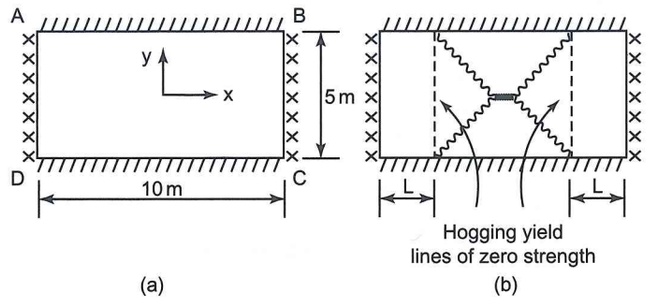

FIGURE P.19.7

moment of resistance from the built in edges so that the ultimate load for this pattern is also 14 kN/m^2. Assume that inclined yield lines make an angle of 45° with the x and y axes.

Ans. $m = 24.31$ kNm/m. $L = 1.875$ m.

P.19.8 The reinforced concrete slab shown in Fig. P.19.8 is simply supported on the sides AB, BC, CD and AD and is continuous over the beam EF which is simply supported at E and F. The slab has isotropic sagging moments of resistance m per unit width and a hogging moment of resistance 1.5 m per unit width over the beam EF. If the slab is subjected to an ultimate load of 15 kN/m^2 determine, by consideration of the two yield line patterns shown, the ultimate moment of resistance of the slab and the ultimate moment of resistance of the beam EF.